Tectonics

Supporting Information for

Reverse faulting within a continental plate boundary transform system

Kirk F. Townsend[1], Marin K. Clark[1], Nathan A. Niemi[1]

[1]Department of Earth and Environmental Sciences, University of Michigan, Ann Arbor, MI, USA

Contents of this file

Introduction

This supplemental document contains a summary of laboratory and analytical protocols for analysis of apatite (U-Th)/He thermochronometry, thermochronometric results for each transect, and descriptions of the pre-exhumation thermal histories as inferred from the thermal models and mapped geology. Fourteen supplemental figures showing geologic cross sections and full best-fit thermal histories are included. QTQt thermal modelling input files for each sample are included.

Text S1: Apatite (U-Th)/He Methods

Samples were crushed, sieved, and separated using standard methods to isolate apatite and zircon by exploiting differences in density and magnetic susceptibility. Individual mineral grains were hand-selected under a high-powered binocular microscope to screen for clarity, crystal morphology, and minimal inclusions of other potentially radiogenic minerals. Grains selected for analysis were measured along major and minor axes, photographed, packaged into individual Pt tubes, and analyzed for ^{4}He content using an Australian Scientific Instruments Helium Instrument (Alphachron) at the University of Michigan Thermochronology Laboratory. Apatite grains were heated for 5 minutes at 900°C, whereas zircon grains were heated for 10 minutes at 1200°C. Released ^{4}He was spiked with ^{3}He, and the ^{4}He /^{3}He ratio was measured on a Pfeiffer quadrupole mass spectrometer to determine the quantity of ^{4}He. Following this initial ^{4}He measurement, these analytical procedures were repeated to check for any additional extraction of ^{4}He that might be indicative of micro-inclusions of high-temperature radiogenic minerals that were not observed optically during grain selection. The Durango apatite age standard was also analyzed with our samples to ensure accuracy of measurements of unknown age. After measurement of ^{4}He, apatite grains were dissolved and analyzed for U, Th and Sm concentrations following standard procedures (Reiners & Nicolescu, 2006) using a Thermo Scientific Elements 2 ICP-MS at the University of Arizona Radiogenic Helium Dating Laboratory. Zircon grains were dissolved in Parr bombs and analyzed for U and Th concentrations at the University of Arizona. Individual grain dates were solved for numerically using parent and daughter nuclide concentrations and the age equation, and analytical uncertainties were propagated through the age equation using Monte Carlo methods.

Individual grains were excluded from calculation of mean ages and thermal models following the criteria of Niemi & Clark (2018). Grains with low uranium concentrations are particularly susceptible to age biases that result from uranium-implantation from surrounding U-rich phases (Spiegel et al., 2009), so we exclude grains with uranium concentrations under 5 ppm from thermal models and calculation of mean ages. Outliers were identified using the Q-test at the 90% confidence interval. Using the remaining grain ages, we calculated mean apatite and zircon helium ages for each sample (Table 1). We do not report mean ages for samples with less than three grains remaining after low-U and outlier grains are removed (four ages). Because the observed variability in our (U-Th-[Sm])/He ages for individual samples is larger than the analytical error for single grains, we report mean ages for samples with uncertainty as the standard error of the mean for the multiple grains analyzed (Tables 1 and 2). We consider samples with a standard error greater than 1.0 Ma that is also greater than 20 percent of the mean age to have low reproducibility, and report ranges of individual grain ages instead of mean ages (nine ages). We do not identify any trends in grainsize and age or radiation damage (eU) and age, which can explain some of the variability in individual grain ages from some samples (Flowers et al., 2009; Guenthner et al., 2013; Reiners & Farley, 2001). We also report ranges of individual grain ages instead of mean ages for samples with grain ages that are older than the depositional age of the sedimentary rock from which they were collected, as these ages are likely inherited and do not reflect recent cooling of the sample (14 ages) (Tables 1 and 2).

Text S2: Thermochronometry results by transect

Apatite and zircon helium results from each transect are described here. Results are first presented from the northern boundary from west to east, and second from the southern boundary from west to east.

S2.1 San Cayetano Fault System

S2.1.1 Rattlesnake Canyon Transect

The Rattlesnake Canyon transect is located just north of Santa Barbara, CA in the Santa Ynez Mountains (Figure 2a). The transect includes three samples that span 2,100 meters of stratigraphic separation in the hanging wall of the Santa Ynez Fault, with stratigraphic depth increasing with proximity to the fault (Figure S1). Samples were collected from Cretaceous through Oligocene sandstones (Dibblee & Ehrenspeck, 1986), and AHe ages are 2.0 ± 0.1 Ma, 3.0 ± 0.1 Ma, and 3.8 ± 0.3 Ma (Table 1). These ages exhibit an age-stratigraphic depth trend, but not an age-elevation trend. ZHe analyses from the stratigraphically lowest sample (18-SBRC-7), closest to the Santa Ynez Fault, yielded a mean age of 15.3 ± 0.6 Ma (Table 1).

S2.1.2 Matilija Canyon Transect

The Matilija Canyon transect is located along the Ventura River and North Fork Matilija Creek north of Ojai, CA, in the eastern Santa Ynez Mountains. The transect includes seven samples that span 3,500 meters of stratigraphic separation in the hanging wall of the Santa Ynez Fault, with stratigraphic depth increasing with proximity to the fault (Figure S2). All samples were collected from Cretaceous through Oligocene sandstones (Dibblee, 1985, 1987a), and AHe ages range from 1.6 ± 0.2 Ma to 2.9 ± 0.3 Ma. ZHe analyses on five of these seven samples yield mean ages that range from 17.7 ± 3.1 Ma to 35.3 ± 0.7 Ma. ZHe analyses on the stratigraphically highest sample (16-OJ-1) yielded individual grain ages that range from 52.0 to 71.4 Ma, which are older than the Late-Eocene depositional age of the Coldwater Sandstone from which the sample was collected. Both the AHe and ZHe analyses demonstrate age-stratigraphic relationships, but no age-elevation trend (Table 1). White (1991) reports a mean apatite fission track age of 2.0 ± 1.2 Ma from sample WG2-90, which was collected from the sample outcrop as 17-OJ-7 (AHe age of 2.0 ± 0.5 Ma). The pooled apatite fission-track age and track length distribution of this samples was incorporated into the thermal models of this transect.

S2.1.3 Sisar Canyon Transect

The Sisar Canyon transect is located northeast of Ojai, CA at the boundary between the Santa Ynez and Topatopa Mountains. Here the predominantly east-west striking, near-vertical homocline of the Santa Ynez Mountains and the generally north-south striking, gently east-dipping homocline of the Topatopa Mountains intersect in a structurally-complex series of plunging folds. Although maximum depth of exposure (Cretaceous) is higher in the Santa Ynez Mountains than the Topatopa Mountains, the Eocene through Miocene units are largely the same in both ranges. Due to the relatively complicated structural setting, samples were collected with elevation separation instead of stratigraphic separation. Four samples that span 1,200 meters of elevation separation were collected from Eocene sandstones in the hanging wall of the San Cayetano Fault (Dibblee, 1987b, 1990). AHe ages range from 2.1 ± 0.1 Ma to 3.4 ± 0.01 Ma and exhibit an age-elevation trend (Figure S9). ZHe analyses conducted on the second-lowest sample (18-OSC-5) yielded individual grain ages ranging from 11.8 Ma to 40.5 Ma.

S2.1.4 Santa Paula Canyon Transect

The Santa Paula Canyon transect is located in the Topatopa Mountains along Santa Paula Creek north of the community of Santa Paula, CA (Dibblee, 1990). The transect includes two samples collected from Eocene sandstones that span <500m of stratigraphic separation. Mean AHe sample ages are 2.3 ± 0.4 Ma (16-SP-1) and 2.1 ± 0.1 Ma (16-SP-3), and the mean ZHe age from sample 16-SP-3 is 56.3 ± 8.8 Ma (Table 1). Due to the relatively complicated structural setting between strands of the San Cayetano Fault, only the AHe and ZHe data from 16-SP-3 were included in the thermal model.

S2.1.5 Santa Paula Peak Transect

The Santa Paula Peak transect is located in the Topatopa Mountains northeast of Santa Paula, CA and northwest of Fillmore, CA. The transect includes three samples collected from the Eocene Matilija Sandstone, which is tightly folded due to fault-proximal deformation associated with slip on the San Cayetano Fault. These samples span 750 meters of elevation separation. AHe ages from two samples yield cooling ages of 1.3 ± 0.2 Ma (18-SPP-2) and 2.7 ± 0.3 Ma (18-SPP-3) and exhibit an age-elevation relationship. ZHe analyses from one sample near the base of the transect (18-SPP-6) yielded a mean age of 50.0 ± 7.8 Ma.

S2.1.6 Hopper Mountain Transect

Hopper Mountain transect is located in the central Topatopa Mountains northeast of Fillmore, CA. The transect includes seven samples that span >1,100 meters of elevation separation. Samples were collected from Oligocene through Miocene sandstones and record AHe cooling ages of 1.6 ± 0.2 Ma to 3.3 ± 0.3 Ma. The lowest six samples on the transect yield cooling ages that are within one-sigma uncertainty of each other, and an age-elevation relationship is only apparent after adding the highest-elevation sample (18-FC-1, AHe age of 3.3 ± 0.3 Ma). ZHe analyses performed on four grains from the lowest elevation sample (16-FM-1) yield individual grain dates ranging from 52 to 72 Ma, which are older than the depositional age of the Oligocene Sespe Formation from which the sample was collected.

S2.1.7 Piru Transect

The Piru transect is located north of Piru, CA in the eastern Topatopa Mountains. Five samples were collected at similar elevation but varying stratigraphic depth within the Miocene Monterey Formation (locally known as Modelo Formation; Dibblee, 1991b). Within rejection criteria (Text S1), only one sample (16-PC-2) yielded a mean AHe cooling age younger than the depositional age of the Modelo Formation (5.9 ± 1.0 Ma). Individual grain ages of sample 16-PC-2 range from 1.8 to 27.3 Ma, which likely indicates partial resetting within the Helium partial retention zone. ZHe analyses were conducted on two samples, and resultant grain ages range from 75 to 89 Ma (16-PC-2) and 64 to 86 Ma (16-PC-4). These ZHe cooling ages are older than the depositional age of the formation, indicating that they do not record a cooling event related to recent exhumation. We were unable to solve for unique time-temperature histories with thermal modeling due to the lack of separation of AHe samples or reset ZHe ages. However, despite the high dispersion of in individual grains ages, young AHe grain ages of < 2.0 Ma in sample 16-PC-2 likely record both recent and rapid cooling due to exhumation.

S2.2 Santa Monica-Channel Islands Fault System

S2.2.1 Northern Channel Islands

Six samples were collected on a stratigraphic transect of Eocene through Miocene strata in the central and southern portions of Santa Rosa Island. Samples span 1,000 meters of stratigraphic separation, and AHe analyses on all but the stratigraphically highest sample yield mean ages ranging from 6.4 ± 0.1 to 9.6 ± 1.5 Ma. The stratigraphically highest sample (18-SRI-2) yielded grain ages ranging from 12.0 to 34.3 Ma, which are within the early-Miocene depositional age of the Rincon Formation from which it was collected, indicating that this sample was likely only partially reset during burial. Therefore, it was excluded from the thermal models. Sample 18-SCI-9 was also excluded from thermal modelling as it was collected from a fault-bounded block of South Point Sandstone with no marker horizons or unit contacts with which to place the sample in stratigraphic context. ZHe analyses from the stratigraphically lowest sample (18-SCI-6) yielded grain ages ranging from 51 to 85 Ma, which are older than the Middle-Eocene depositional age of the South Point Sandstone from which it was collected.

Seven samples were collected from the Paleocene through Miocene section of sedimentary rocks on the southwest end of Santa Cruz Island, to the east of Santa Rosa Island (Figures 1 and 3, Table 2). AHe analyses from one sample (18-PS-3) yielded a relatively young cooling age of 7.0 ± 0.6 Ma, which is consistent with cooling ages from Santa Rosa Island (Tables 1 and 2). Three samples (18-PS-1, 18-PS-7, and 18-PS-8) yielded cooling ages that are within or older than the depositional ages of the Miocene strata from which they were collected, indicating that they likely did not experience temperatures high enough during burial to reset the detrital thermal ages. AHe analyses from the Eocene and Paleocene strata yield cooling ages ranging from 18.2 ± 2.3 Ma to 29.5 ± 2.7 Ma. These samples do not exhibit age-stratigraphic depth or age-elevation relationships, and we therefore do not produce thermal models with these data.

S2.2.2 Zuma Ridge and Las Flores Canyon Transects

AHe and ZHe data from the Las Flores Canyon and Zuma Ridge transects were produced by Niemi & Clark (2018). These transects span 1,600 meters (Las Flores Canyon) and 900 meters (Zuma Ridge) of stratigraphic separation and are located in the central Santa Monica Mountains near Malibu, CA. AHe ages of eight samples from Las Flores Canyon range from 2.3 to 11.5 Ma, and AHe ages of thirteen samples from Zuma Ridge range from 4.5 to 12.6 Ma. AHe ages exhibit both age-stratigraphic depth and age-elevation trends. ZHe ages from three samples on these transects range from 36 to 61 Ma.

S2.2.3 Hollywood Transect

The Hollywood transect is located in the Hollywood Hills north of downtown Los Angeles, CA and spans 2,400 meters of stratigraphic separation. AHe analyses were conducted on two samples collected from a Cretaceous quartz diorite at the base of the transect, one sample collected from a Cretaceous sandstone that nonconformably overlies the quartz diorite, and four samples collected from Miocene sandstones and conglomerates that disconformably overlie the Cretaceous sandstone (Dibblee, 1991a). AHe ages from the basal quartz diorite and overlying Cretaceous strata range from 2.6 ± 0.4 Ma to 8.6 ± 1.3 Ma, and AHe ages from the Miocene section range from 7.1 ± 0.8 Ma to 20.4 ± 0.7 Ma. ZHe analyses conducted on the lowest sample yield a mean age of 22.1 ± 1.5 Ma. AHe data demonstrate an age-stratigraphic depth relationship, but mean AHe ages of samples collected from the Miocene strata are within the

depositional age of these units. We included samples from Miocene rocks in the thermal model to produce predicted thermal histories, but these samples were not used in the inversion for most-likely thermal histories (Figure 4).

Text S3: Post-Deposition Thermal Histories

Prior to late-Miocene time, thermal histories are mostly informed by the depositional history of the stratigraphic units from which samples were collected (Figures S4-S14). On the San Cayetano fault system, the Rattlesnake Canyon and Matilija Canyon transects record slow burial in Cretaceous through late-Eocene time (Figures S4 and S6). Thermal histories from the Sisar Canyon (Figure S9), Santa Paula Canyon (Figure S10), and Santa Paula Peak (Figure S11) transects record rapid burial beginning in late-Eocene through late-Miocene time, which is consistent with deposition of the Juncal Formation, Matilija Sandstone, Cozy Dell Shale, and Coldwater Sandstone in middle- to late-Eocene time, the Sespe Formation in Oligocene time, and the Monterey Formation in Miocene-time. Oligocene to middle- to late-Miocene strata were sampled at Hopper Mountain, and the thermal history (Figure S12) records relatively slow burial in Oligocene through middle-Miocene time, followed by rapid burial in late-Miocene through Pliocene time. This rapid burial is consistent with deposition of the Modelo Formation (time-equivalent of the Monterey Formation) in a localized transtensional basin (Gordon, 2014).

Sedimentation along the Santa Monica-Channel Islands fault system was interrupted by the development of regional unconformities. After initial cooling of the Cretaceous pluton at the base of the sampling transect in Hollywood (Figure S13), the thermal history records cooling from Eocene through Early-Miocene time, which is likely a consequence of erosion of overlying strata and is reflected in the geologic record as a disconformable contact between the Cretaceous strata (Unnamed) and the overlying Miocene units (Middle and Upper Topanga Formations). This phase of cooling was followed by rapid re-heating through late-Miocene time, which is consistent with deposition of the overlying middle- to late-Miocene strata. The Zuma ridge transect similarly records a cooling event from Eocene through Oligocene time, followed initially by slow reheating due to burial of Oligocene units, and more rapid reheating due to burial of Miocene strata (Niemi & Clark, 2018). However, the Las Flores Canyon transect record relatively constant heating due to burial from early-Eocene through latest-Miocene time (Niemi & Clark, 2018). The Santa Rosa Island transect records slow heating due to burial in Oligocene through early-Miocene time, followed by more rapid heating due to burial until late-Miocene time (Figure S14).

References Cited in Supporting Information

Dibblee, T. W. (1985). *Geologic Map of the Wheeler Springs Quadrangle, Ventura County, California*. Santa Barbara, California: Dibblee Geological Foundation.

Dibblee, T. W. (1987a). *Geologic Map of the Matilija Quadrangle, Ventura County, California*. Santa Barbara, California: Dibblee Geological Foundation.

Dibblee, T. W. (1987b). *Geologic Map of the Ojai Quadrangle, Ventura County, California*. Santa Barbara, California: Dibblee Geological Foundation.

Dibblee, T. W. (1990). Geologic Map of the Santa Paula Peak Quadrangle. *Santa Barbara Museum of Natural History*.

Dibblee, T. W. (1991a). *Geologic Map of the Hollywood and South 1/2 Burbank Quadrangles*. Santa Barbara, California: Dibblee Geological Foundation.

Dibblee, T. W. (1991b). *Geologic Map of the Piru Quadrangle, Ventura County, California*.

Santa Barbara, California: Dibblee Geological Foundation.
Dibblee, T. W., & Ehrenspeck, H. E. (1986). *Geologic map of the Santa Barbara quadrangle, Santa Barbara County, California*. Santa Barbara, California: Dibblee Geological Foundation.
Flowers, R. M., Ketcham, R. A., Shuster, D. L., & Farley, K. A. (2009). Apatite (U-Th)/He thermochronometry using a radiation damage accumulation and annealing model. *Geochimica et Cosmochimica Acta*, *73*(8), 2347–2365. https://doi.org/10.1016/j.gca.2009.01.015
Gordon, G. (2014). *Stratigraphic evolution and architectural analysis of structurally confined submarine fans: A tripartite outcrop-based study*. Colorado School of Mines.
Guenthner, W. R., Reiners, P. W., Ketcham, R. A., Nasdala, L., & Giester, G. (2013). Helium diffusion in natural zircon: radiation damage, anisotropy, and the interpretation of zircon (U-TH)/He thermochronology. *American Journal of Science*, *313*(3), 145–198. https://doi.org/10.2475/03.2013.01
Niemi, N. A., & Clark, M. K. (2018). Long-term exhumation rates exceed paleoseismic slip rates in the central Santa Monica Mountains, Los Angeles County, California. *Geology*, *46*(1), 63–66. https://doi.org/10.1130/G39388.1
Reiners, P. W., & Farley, K. A. (2001). Influence of crystal size on apatite (U-Th)/He thermochronology: An example from the Bighorn Mountains, Wyoming. *Earth and Planetary Science Letters*, *188*(3–4), 413–420. https://doi.org/10.1016/S0012-821X(01)00341-7
Reiners, P. W., & Nicolescu, S. (2006). Measurement of parent nuclides for (U-Th)/He chronometry by solution sector ICP-Ms. *ARDHL Report 1*, (December 2006), 1–33. Retrieved from http://www.geo.arizona.edu/~reiners/arhdl/arhdl.html
Spiegel, C., Kohn, B., Belton, D., Berner, Z., & Gleadow, A. (2009). Apatite (U-Th-Sm)/He thermochronology of rapidly cooled samples: The effect of He implantation. *Earth and Planetary Science Letters*, *285*(1–2), 105–114. https://doi.org/10.1016/j.epsl.2009.05.045

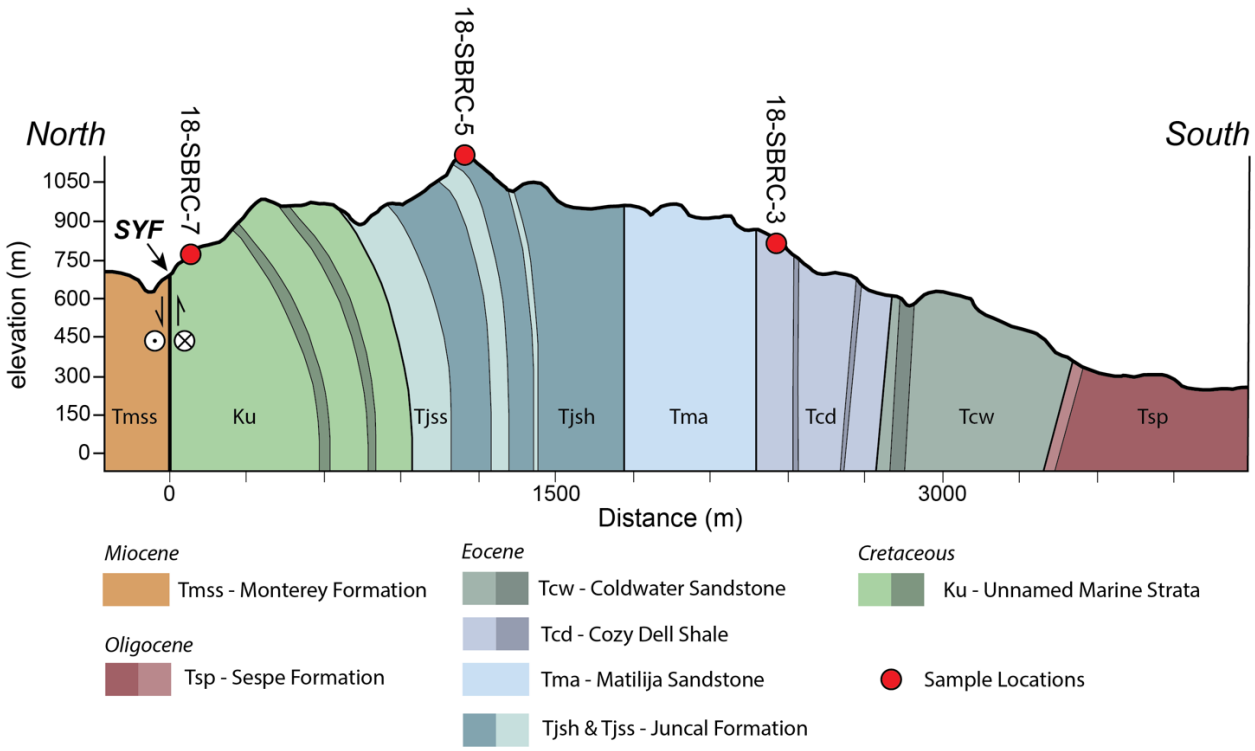

Figure S1. Cross section through the Santa Ynez anticlinorium at the Rattlesnake Canyon transect. Cross section interpreted from Dibblee & Ehrenspeck (1986). SYF–Santa Ynez Fault. Note that Eocene (Tjsh, Tma, Tcd, Tcw) and Oligocene (Tsp) strata are locally overturned, and that stratigraphic up within the Santa Ynez anticlinorium is towards the south.

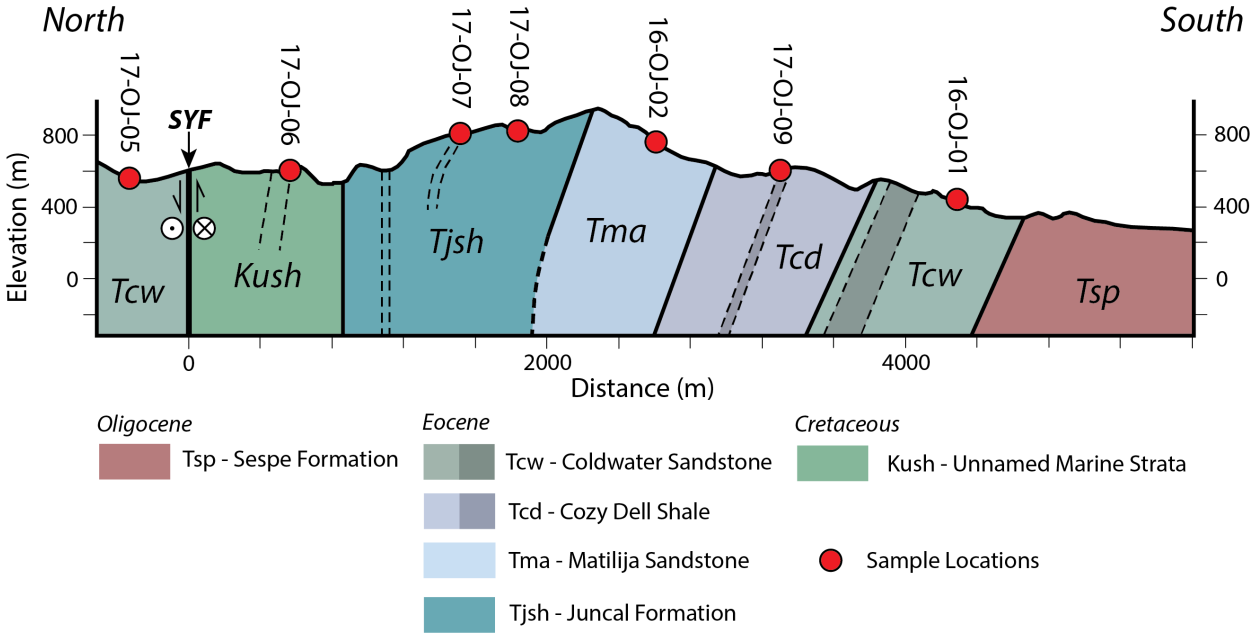

Figure S2. Cross section through the Santa Ynez anticlinorium at the Matilija Canyon transect. Cross section interpreted from Dibblee (1987a). SYF–Santa Ynez Fault. Note that Eocene (Tjsh, Tma, Tcd, Tcw) and Oligocene (Tsp) strata are overturned, and that stratigraphic up within the Santa Ynez anticlinorium is towards the south.

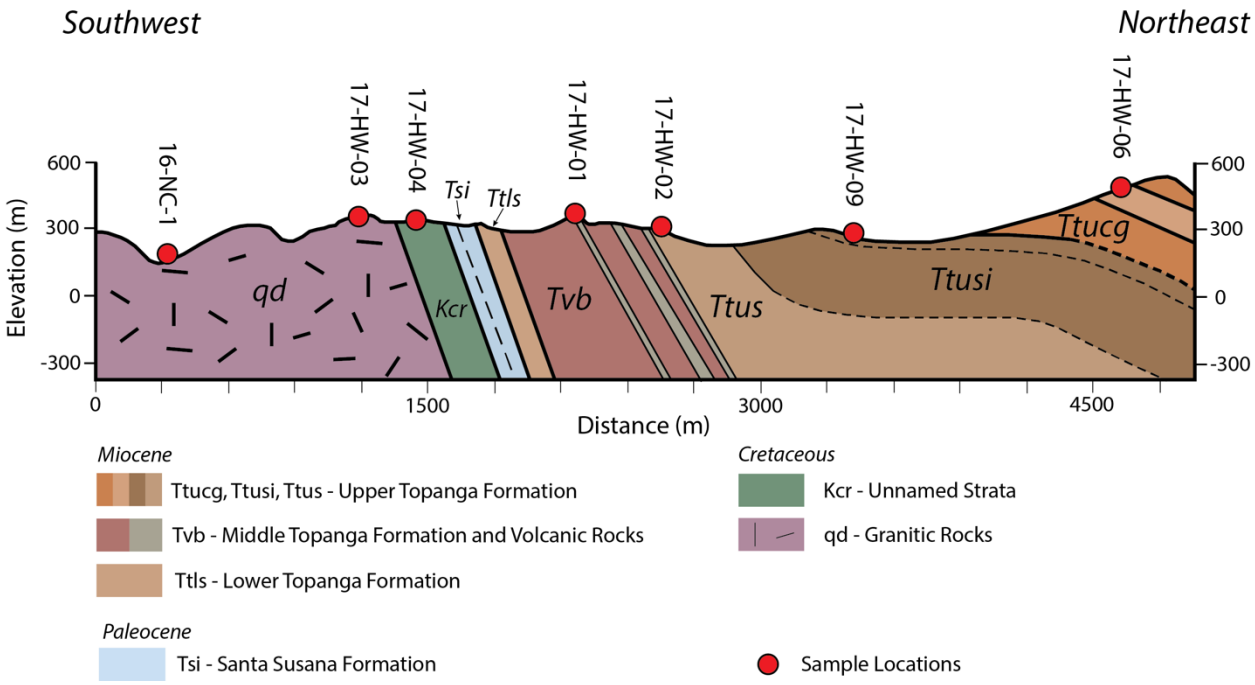

Figure S3. Cross section through the Hollywood Hills at the Hollywood transect. Miocene strata and volcaniclastic rocks disconformably overlie the Paleocene and Cretaceous strata, which in turn nonconformably overlies the quartz diorite (stratigraphic up is to the northeast). Cross section interpreted from Dibblee (1991b).

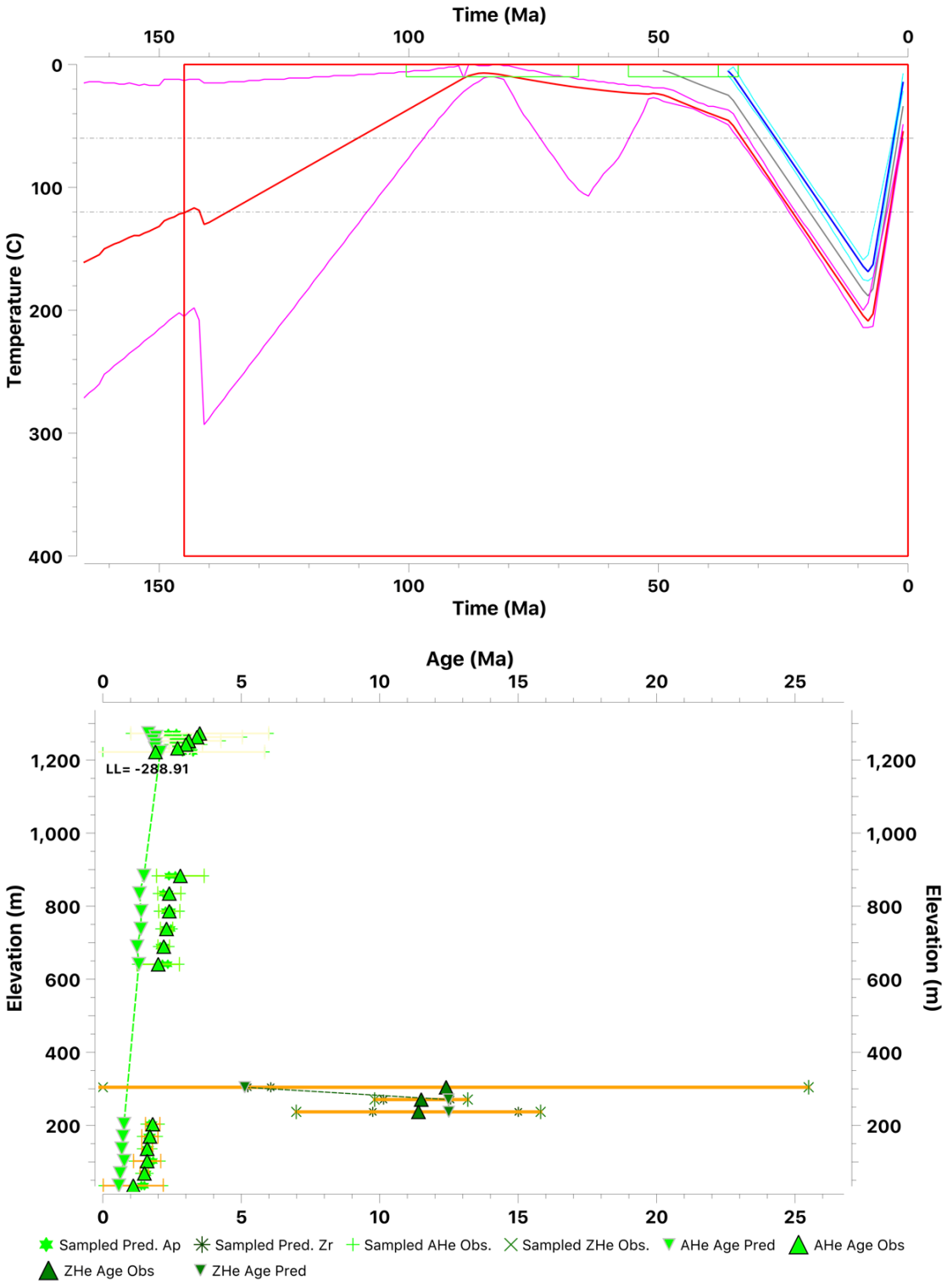

Figure S4. Preferred thermal modelling results for the Rattlesnake Canyon transect data, with vertical sample separation defined by rotating the stratigraphic section back 55 degrees. Top: expected time-temperature history. The red box defines the range of time and temperatures explored in the MCMC. Bottom: Age-elevation plot of observed and predicted thermochronometry sample ages.

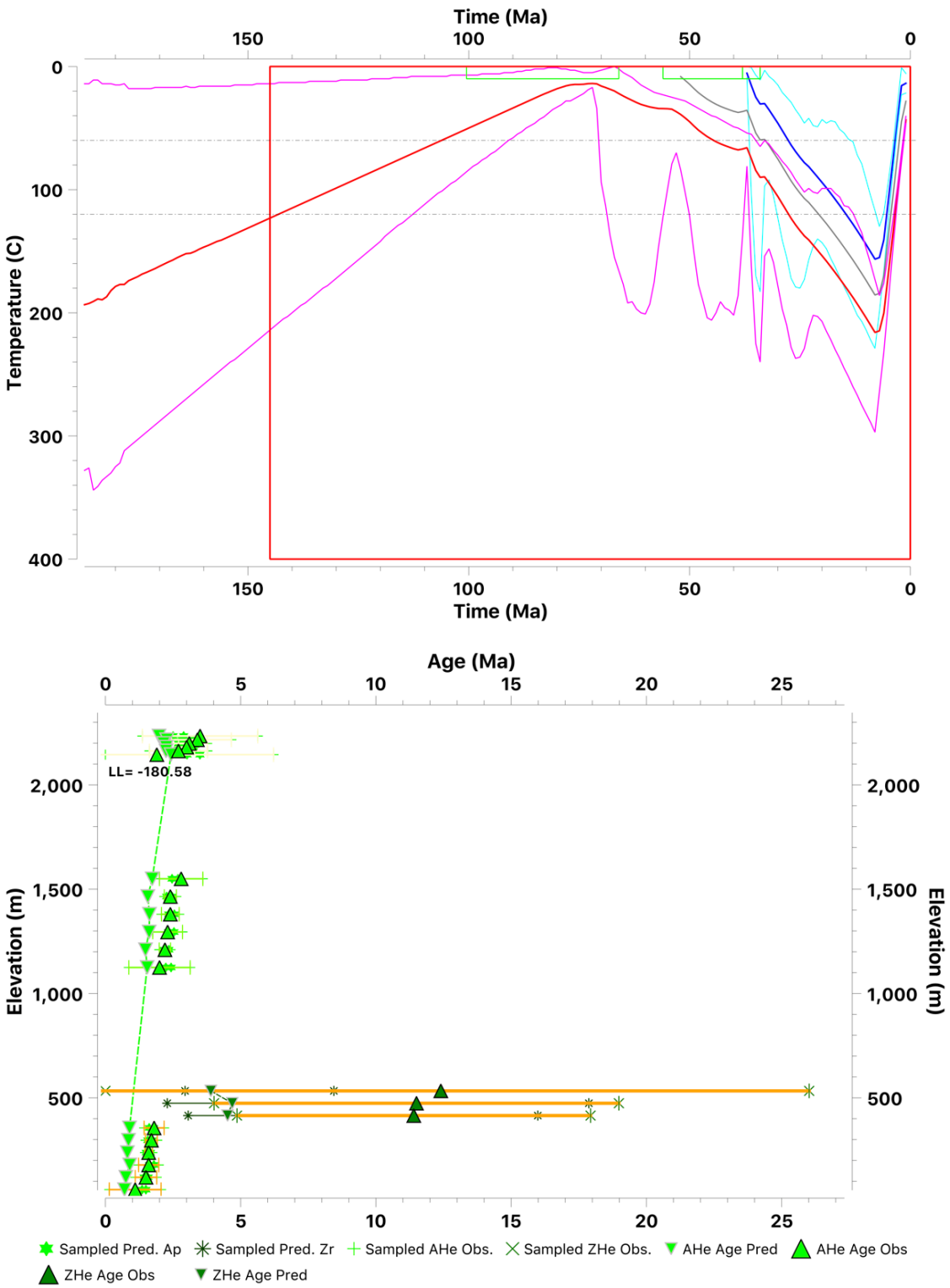

Figure S5. Rattlesnake Canyon transect thermal modelling results with vertical sample separation defined by stratigraphic separation. Top: expected time-temperature history. The red box defines the range of time and temperatures explored in the MCMC. Bottom: Age-elevation plot of observed and predicted thermochronometry sample ages. Modelled ages of zircon thermochronometry samples underpredict observed ages.

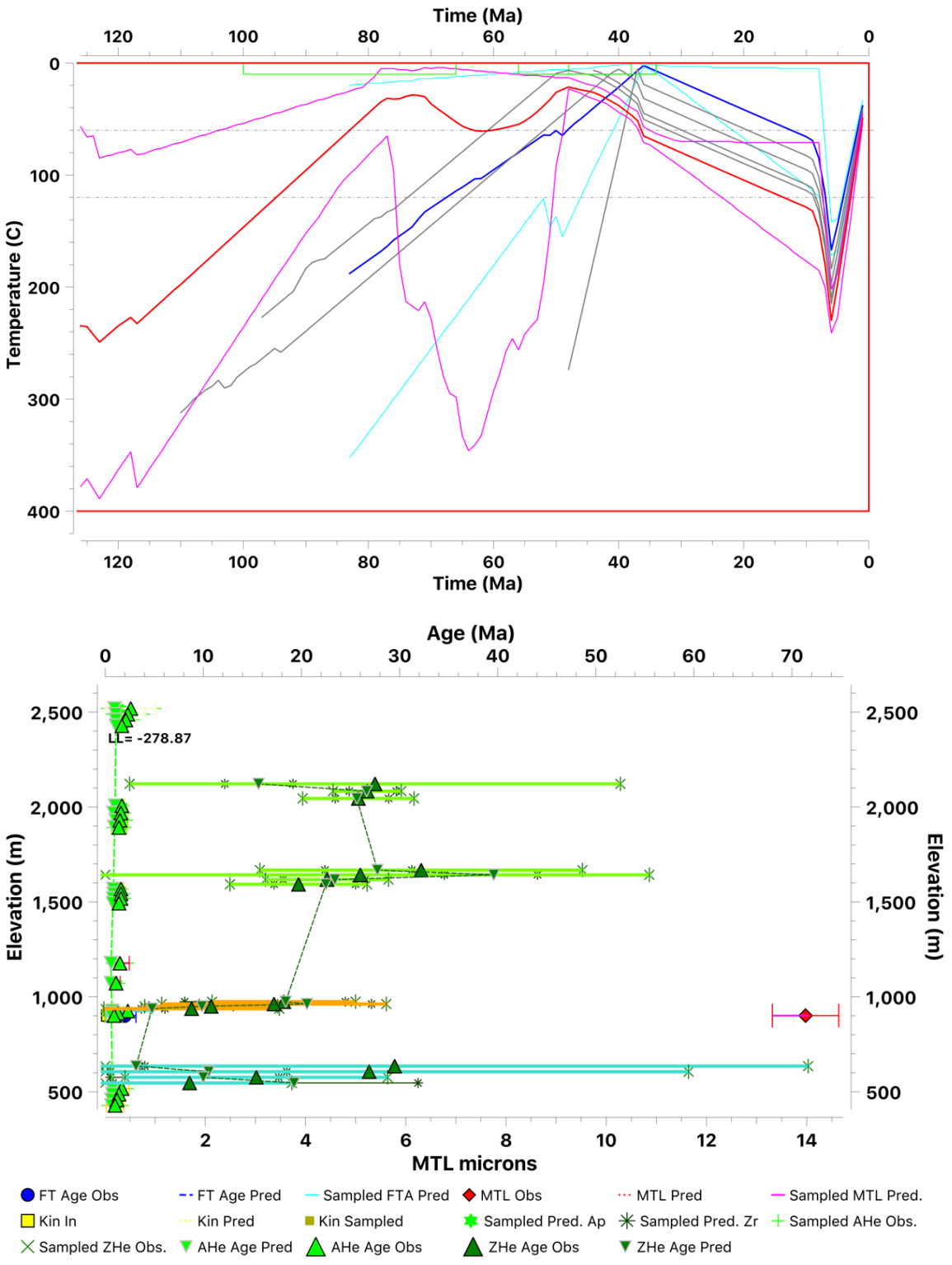

Figure S6. Preferred thermal modelling results for the Matilija Canyon transect data, with vertical sample separation defined by rotating the stratigraphic section back 55 degrees. Top: expected time-temperature history. The red box defines the range of time and temperatures explored in the MCMC. Bottom: Age-elevation plot of observed and predicted thermochronometry sample ages.

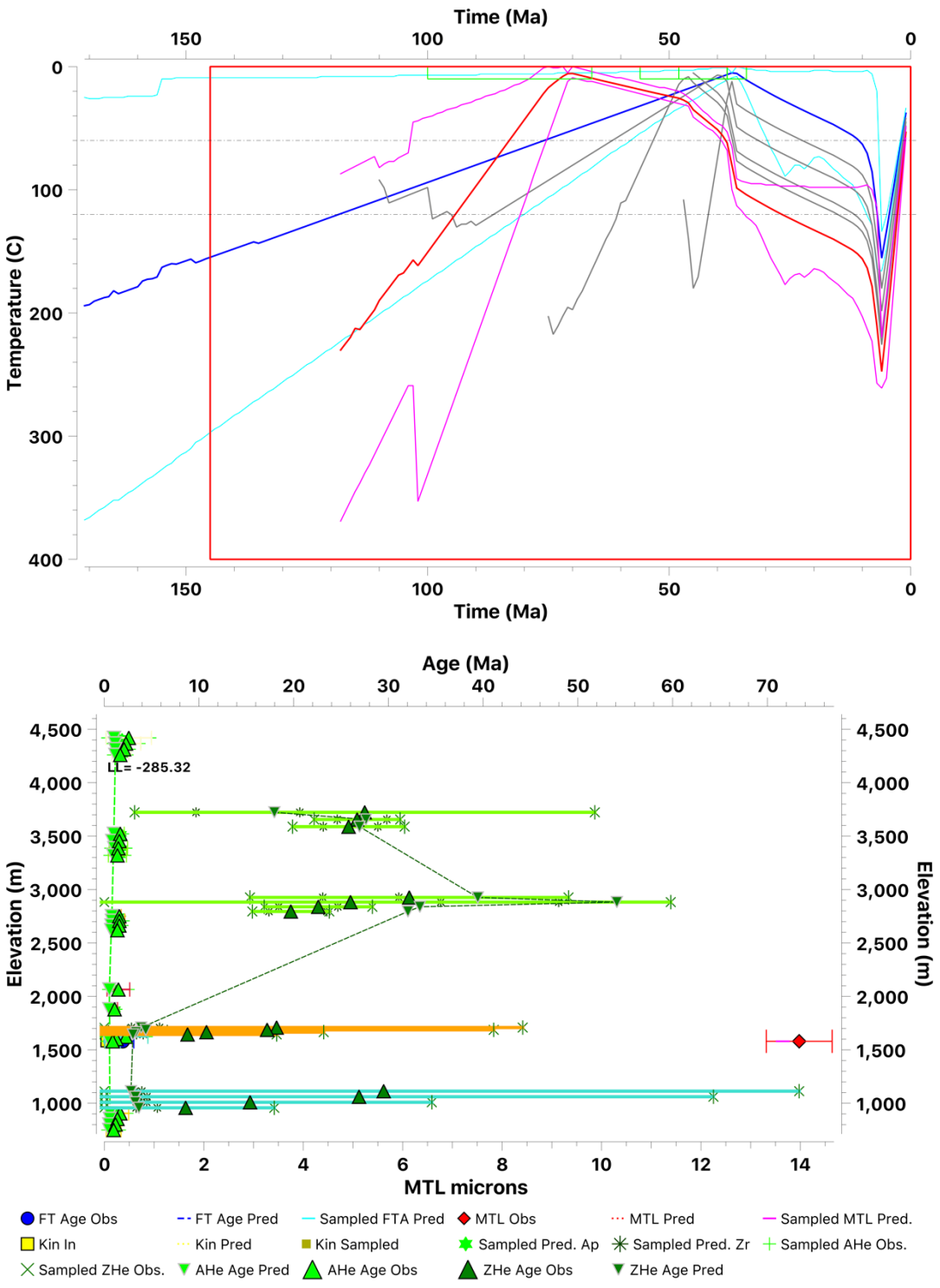

Figure S7. Thermal modelling results for the Matilija Canyon transect data, with vertical spacing defined by stratigraphic separation. Top: expected time-temperature history. The red box defines the range of time and temperatures explored in the MCMC. Bottom: Age-elevation plot of observed and predicted thermochronometry sample ages. Modelled ages of lower two zircon thermochronometry samples underpredict observed ages.

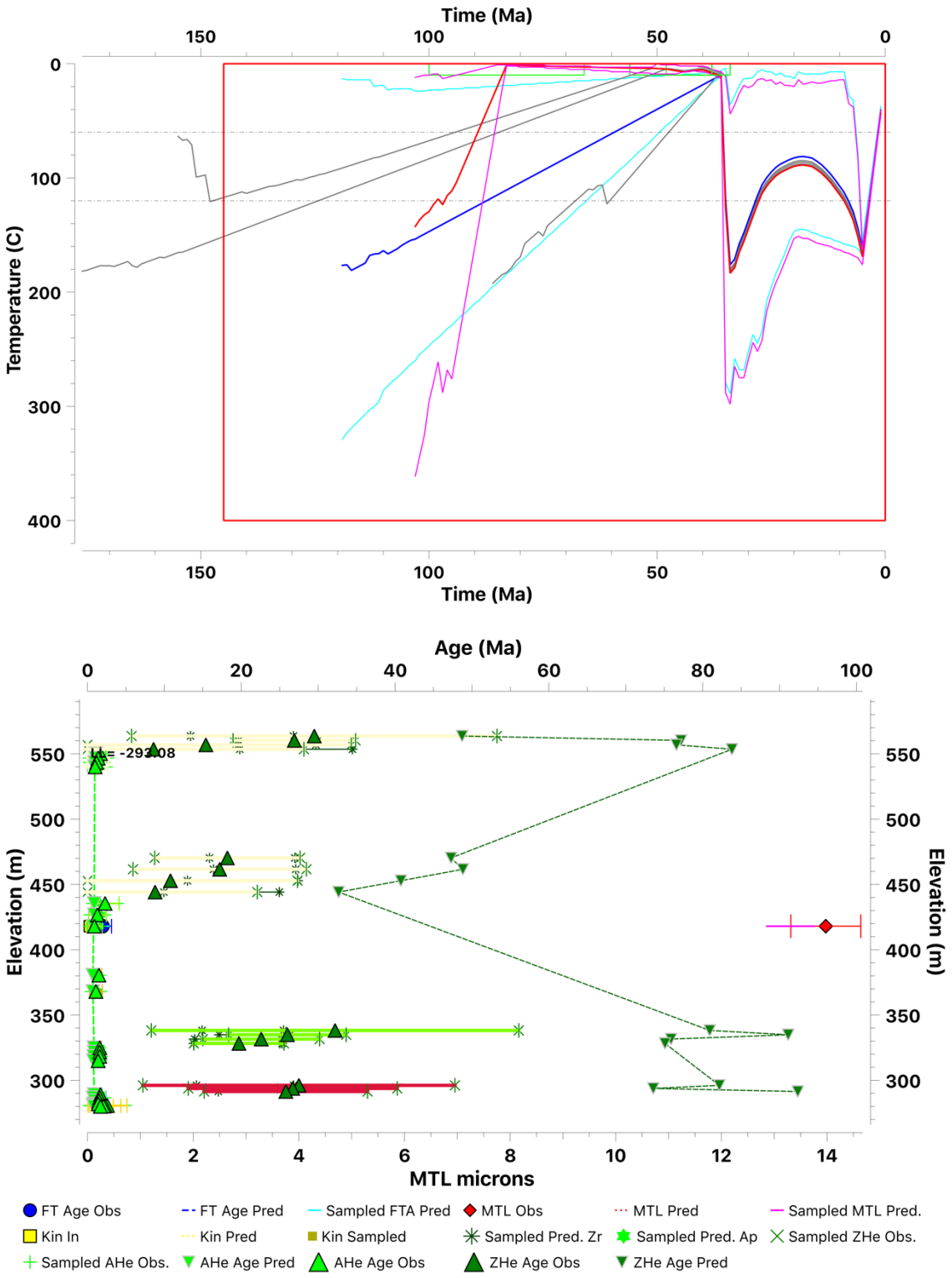

Figure S8. Thermal modelling results for the Matilija Canyon transect data, with vertical spacing defined by elevation. Top: expected time-temperature history. The red box defines the range of time and temperatures explored in the MCMC. Bottom: Age-elevation plot of observed and predicted thermochronometry sample ages. Modelled zircon thermochronometry ages overpredict observed ages.

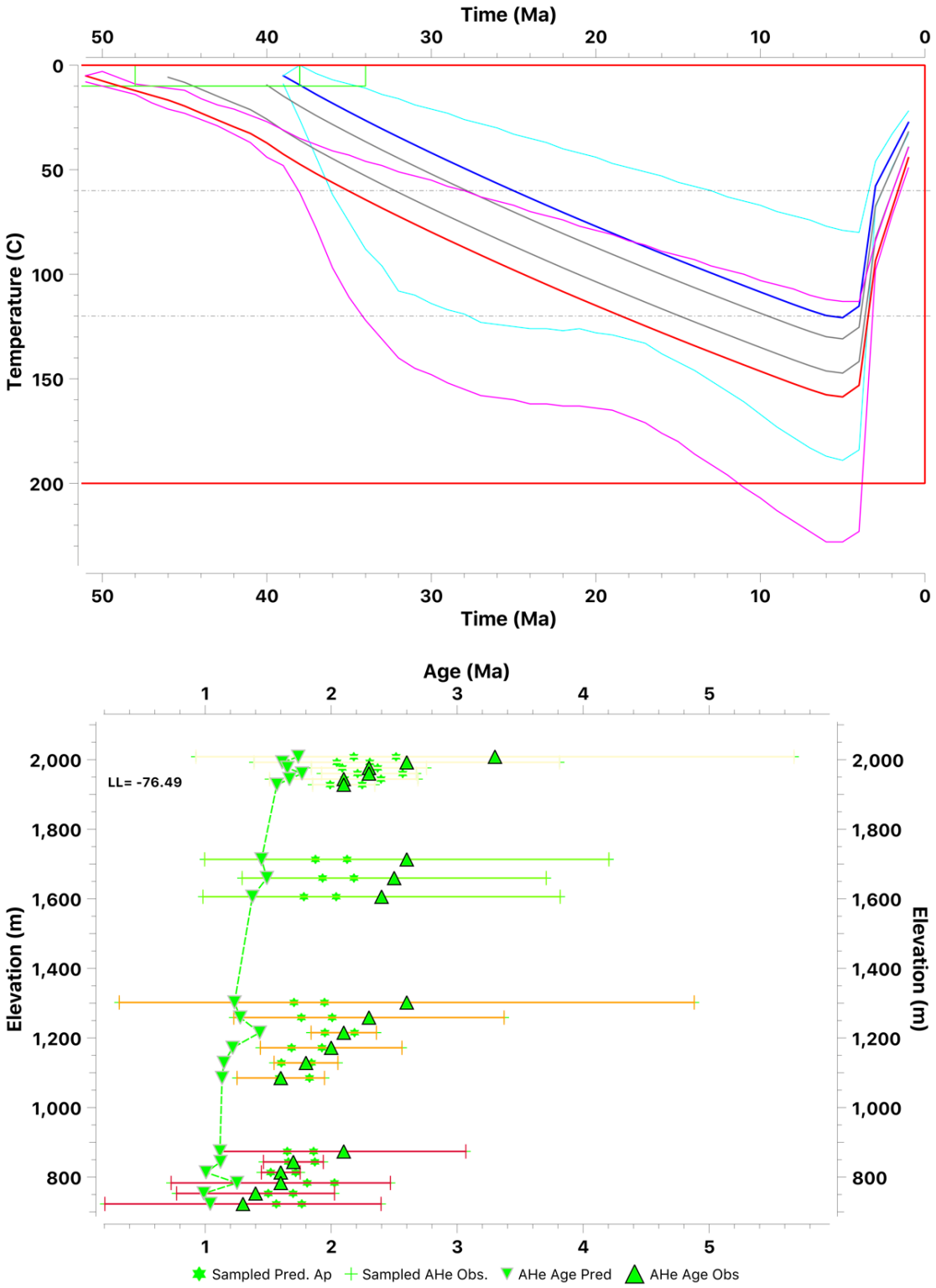

Figure S9. Sisar Canyon transect thermal modelling results. Top: expected time-temperature history. The red box defines the range of time and temperatures explored in the MCMC. Bottom: Age-elevation plot of observed and predicted thermochronometry sample ages.

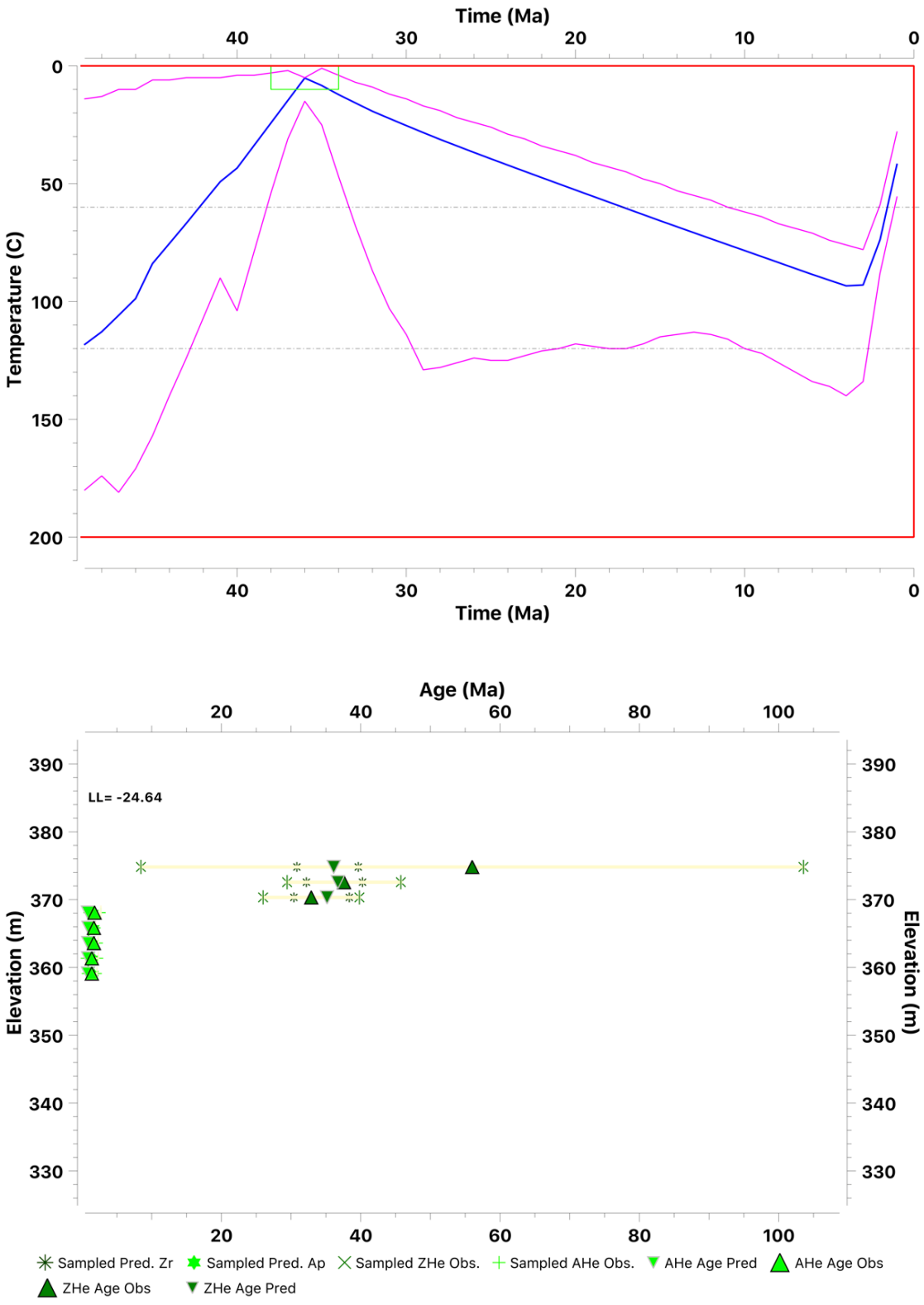

Figure S10. Santa Paula Canyon transect thermal modelling results. Top: expected time-temperature history. The red box defines the range of time and temperatures explored in the MCMC. Bottom: Age-elevation plot of observed and predicted thermochronometry sample ages.

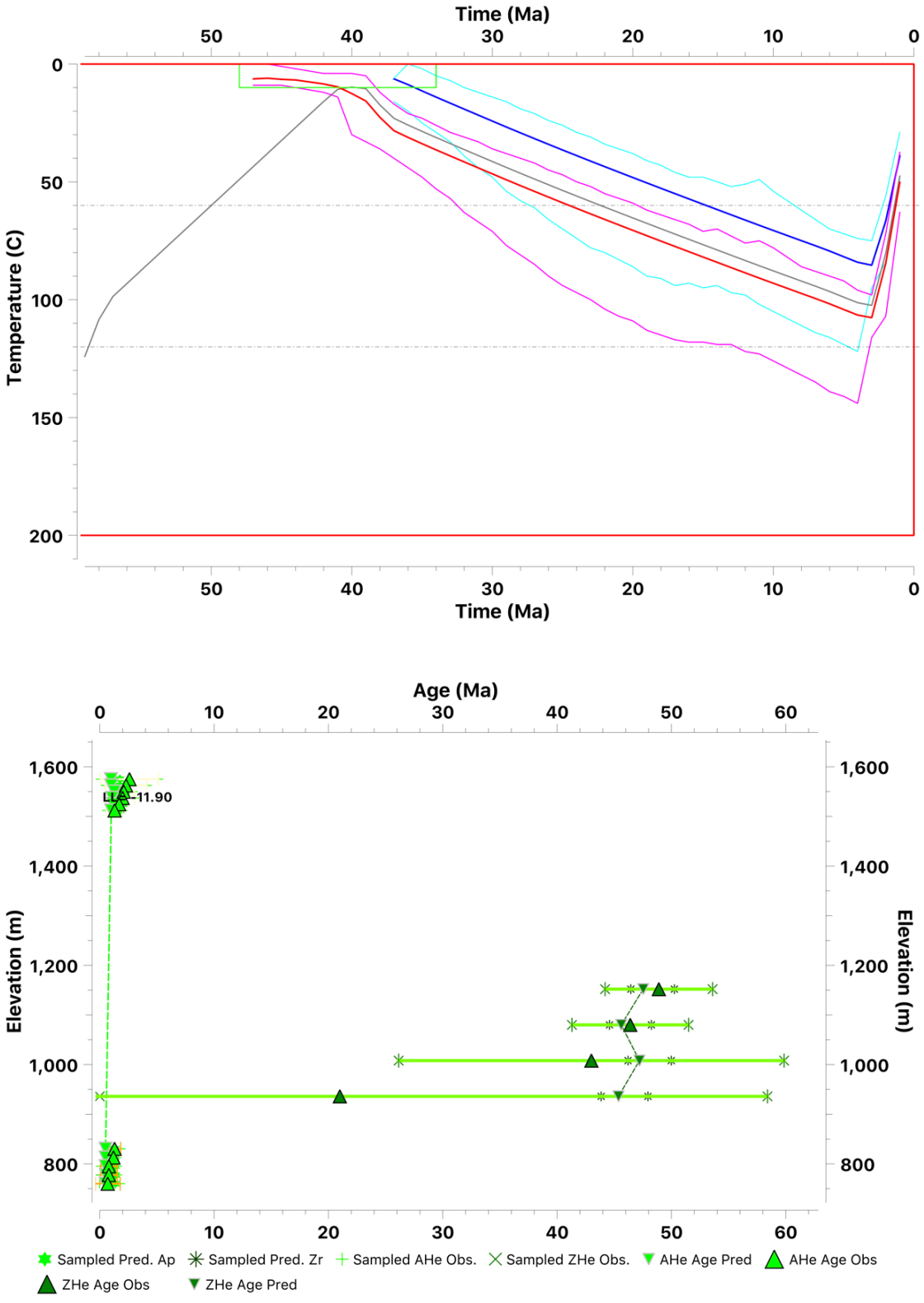

Figure S11. Santa Paula Peak transect thermal modelling results. Top: expected time-temperature history. The red box defines the range of time and temperatures explored in the MCMC. Bottom: Age-elevation plot of observed and predicted thermochronometry sample ages.

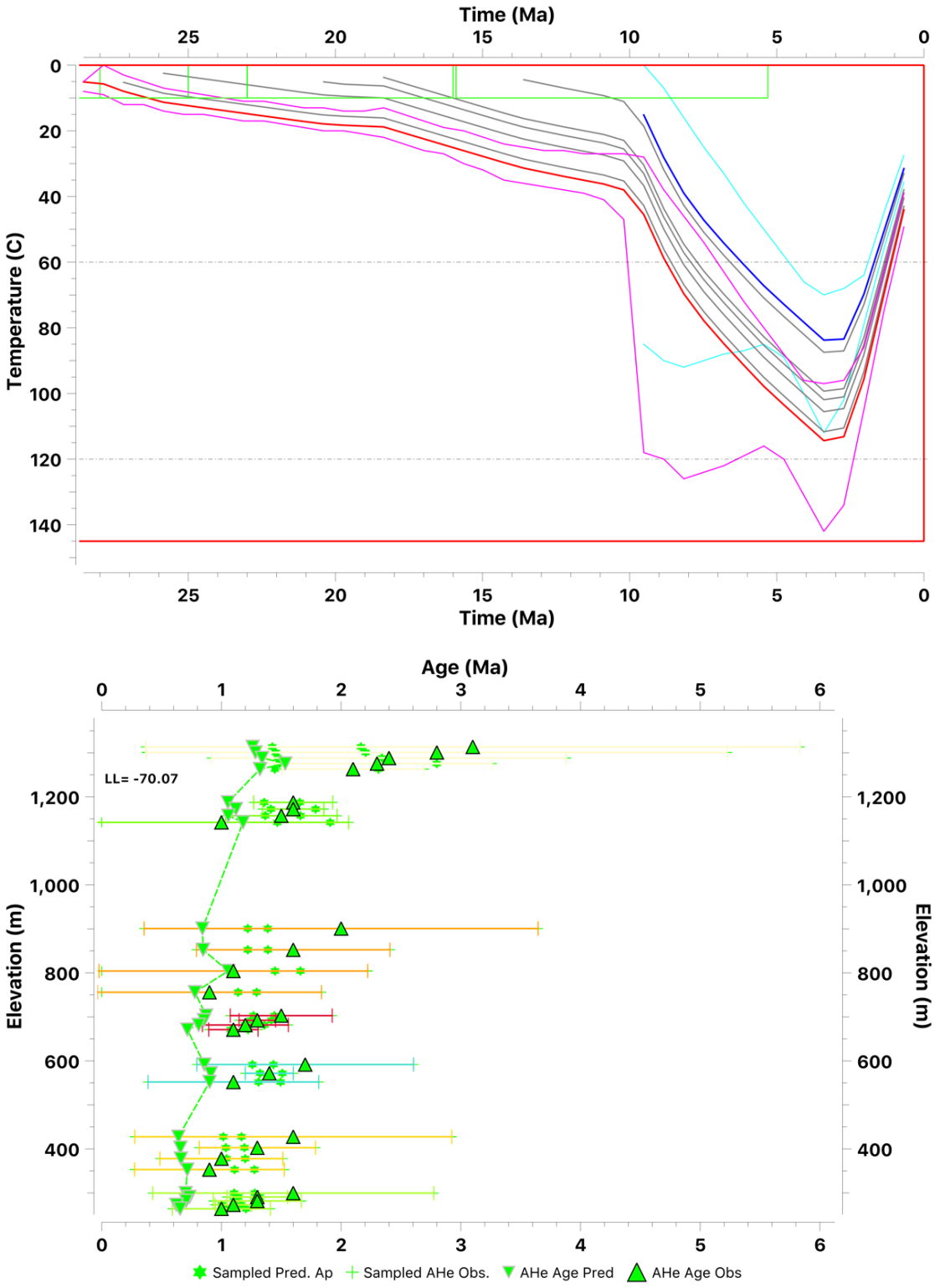

Figure S12. Hopper Mountain transect thermal modelling results. Top: expected time-temperature history. The red box defines the range of time and temperatures explored in the MCMC. Bottom: Age-elevation plot of observed and predicted thermochronometry sample ages.

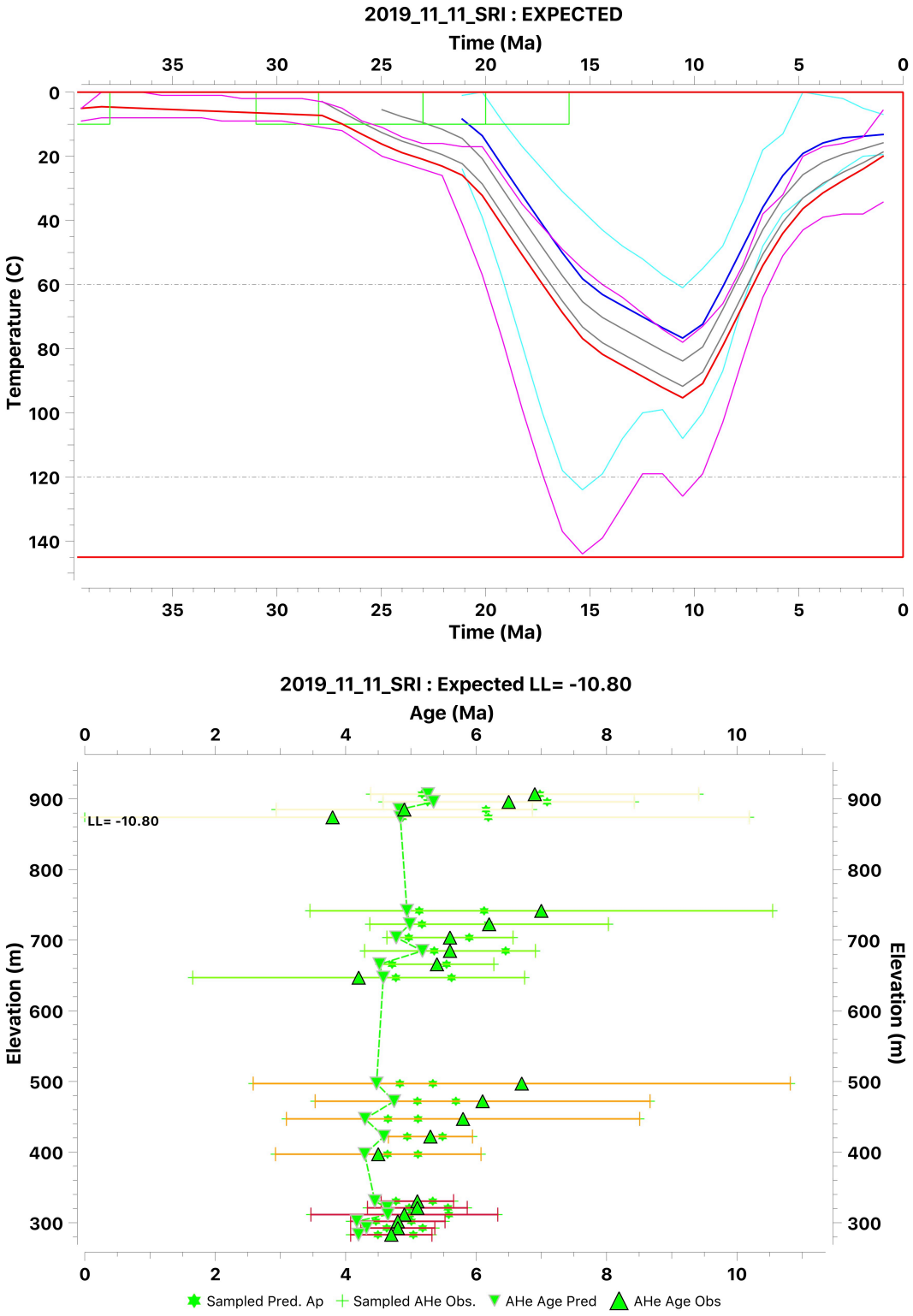

Figure S13. Santa Rosa Island transect thermal modelling results. Top: expected time-temperature history. The red box defines the range of time and temperatures explored in the MCMC. Bottom: Age-elevation plot of observed and predicted thermochronometry sample ages.

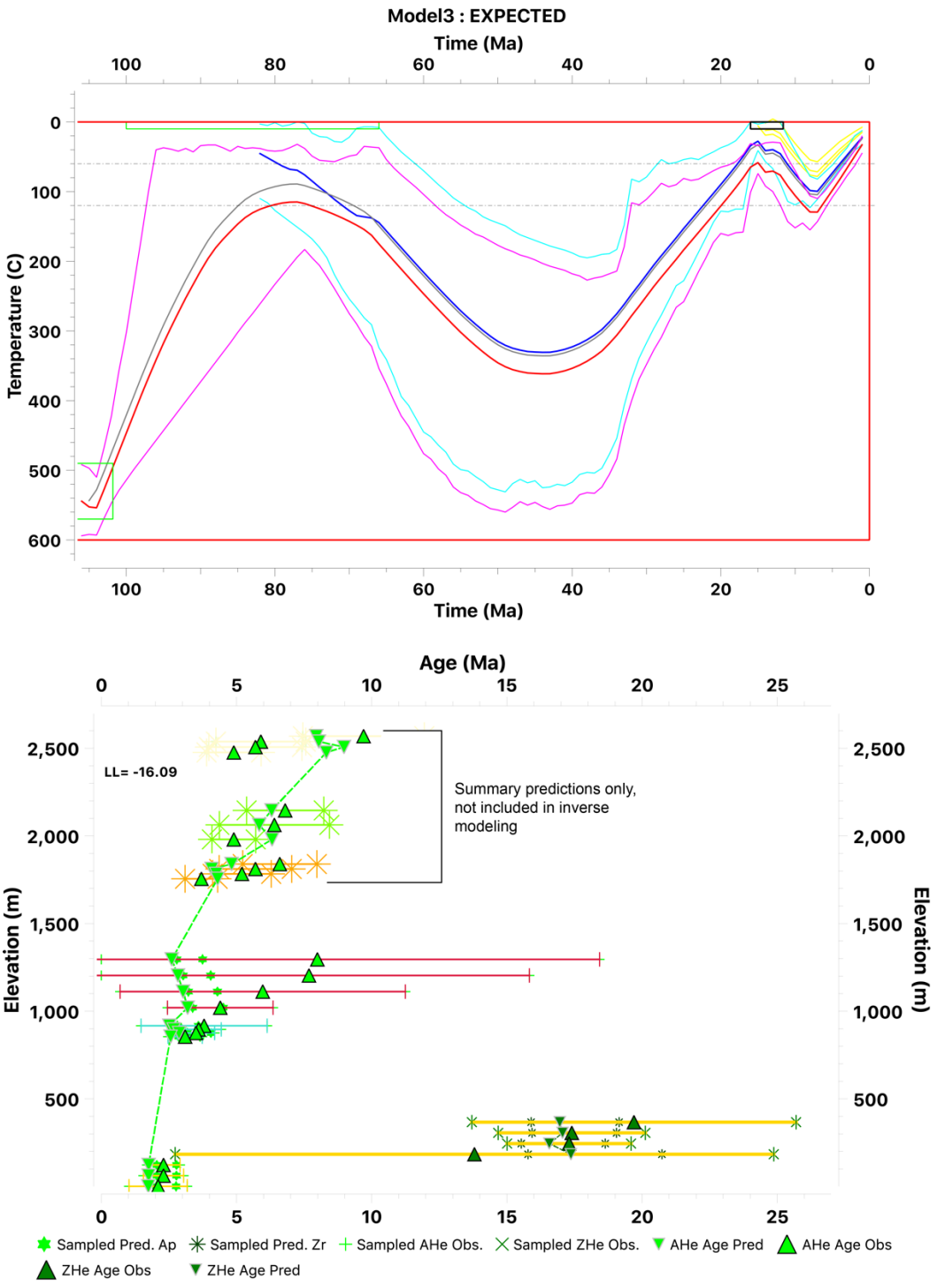

Figure S14. Hollywood transect thermal modelling results. Top: expected time-temperature history. The red box defines the range of time and temperatures explored in the MCMC. The model was constrained to surface temperature in Middle-Miocene time due to the nonconformable contact between Cretaceous and overlying Miocene strata. Yellow lines show predicted thermal histories of three samples from the Middle-Miocene strata, which were not used in the inversion. Bottom: Age-elevation plot of observed and predicted thermochronometry sample ages. Predicted ages of Middle-Miocene strata are shown against observed ages.

QTQt Data Files for Modeled Samples from the Rattlesnake Canyon Transect
Vertical Sample Spacing Set by Stratigraphic Separation

```
18-SBRC-03
0 0 1222
1 0 0 0 0 0
105
0 2 0
1 16.3
0
0
1
-36 -2 5 4.99
0.00 0
0.00 0
0.000 0
6
0
0.02 15.94 60.35 95.59 3.50 -0.04 88.300 98.60 98.60
A 20.44 0.0032 138000 0 2 0
0.05 21.46 48.15 95.10 3.40 -0.04 136.900 114.00 114.00
A 20.03 0.0032 138000 0 2 0
0.01 13.42 2.13 69.69 3.10 -0.05 131.200 94.60 94.60
A 18.99 0.0032 138000 0 2 0
0.03 16.63 30.11 146.34 3.00 -0.04 109.500 121.60 121.60
A 19.84 0.0032 138000 0 2 0
0.02 15.52 20.20 127.39 2.70 -0.04 120.100 114.00 114.00
A 19.63 0.0032 138000 0 2 0
0.01 8.60 7.08 26.29 1.90 -0.13 141.300 137.00 137.00
A 19.43 0.0032 138000 0 2 0
```

```
18-SBRC-05
0 0 641
1 0 0 0 0 0
105
0 2 0
1 16.3
0
0
1
-47 -9 5 4.99
0.00 0
0.00 0
0.000 0
6
0
0.11 37.89 59.81 54.66 2.80 -0.03 143.100 145.80 145.80
A 19.80 0.0032 138000 0 2 0
0.02 13.73 18.34 59.94 2.40 -0.04 144.000 120.60 120.60
A 19.68 0.0032 138000 0 2 0
0.06 37.84 71.21 56.09 2.40 -0.03 114.000 122.00 122.00
A 19.92 0.0032 138000 0 2 0
0.06 41.00 51.70 72.99 2.30 -0.03 144.400 118.40 118.40
A 19.66 0.0032 138000 0 2 0
0.05 45.03 87.42 79.63 2.20 -0.03 125.000 100.80 100.80
A 19.94 0.0032 138000 0 2 0
0.02 18.10 47.41 99.25 2.00 -0.03 120.600 114.40 114.40
A 20.14 0.0032 138000 0 2 0
```

```
18-SBRC-07
0 0 35
1 0 0 0 0 0
105
0 2 0
1 16.3
0
0
1
83.25 17.25 5 4.99
0.00 0
0.00 0
0.000 0
9
7
0.02 8.30 26.03 280.32 1.80 -0.02 133.800 124.60 124.60
A 20.11 0.0032 138000 0 2 0
0.03 29.76 62.71 370.60 1.70 -0.02 136.900 112.60 112.60
A 19.92 0.0032 138000 0 2 0
0.03 28.10 61.69 229.94 1.60 -0.02 188.600 92.80 92.80
A 19.99 0.0032 138000 0 2 0
0.03 46.64 74.75 190.57 1.50 -0.02 130.700 91.00 91.00
A 19.79 0.0032 138000 0 2 0
0.06 40.56 96.19 131.83 1.60 -0.02 171.800 115.20 115.20
A 20.08 0.0032 138000 0 2 0
0.01 30.92 75.71 231.23 1.10 -0.02 110.900 87.00 87.00
A 20.08 0.0032 138000 0 2 0
2.10 427.57 190.70 0.00 12.40 -0.16 166.100 94.00 94.00
Z 15.91 19.3188 165000 3 2 0
6.35 1129.54 260.81 0.00 11.50 -0.16 182.500 102.00 102.00
Z 15.79 19.3188 165000 3 2 0
15.23 1697.76 308.47 0.00 11.40 -0.16 250.900 111.40 111.40
Z 15.76 19.3188 165000 3 2 0
```

QTQt Data Files for Modeled Samples from the Matilija Canyon Transect
Vertical Sample Spacing Set by Stratigraphic Separation

```
16-OJ-01
0 0 2428
1 0 0 0 0 0
105
0 2 0
1 16.3
0
0
1
36 2 5 4.99
0.00 0
0.00 0
0.000 0
4
7
0.02 24.70 7.52 81.62 2.60 -0.04 121.900 84.00 84.00
A 19.11 0.0032 138000 0 2 0
0.02 18.63 4.99 337.98 2.30 -0.04 120.100 99.00 99.00
A 18.95 0.0032 138000 0 2 0
0.03 23.04 57.17 93.47 2.10 -0.03 153.700 95.80 95.80
A 20.11 0.0032 138000 0 2 0
0.01 9.95 21.85 91.05 1.70 -0.03 114.000 111.40 111.40
A 19.98 0.0032 138000 0 2 0
```

```
16-OJ-02
0 0 1493
1 0 0 0 0 0
105
0 2 0
1 16.3
0
0
1
41 7 5 4.99
0.00 0
0.00 0
0.000 0
8
7
0.01 18.99 16.91 442.48 1.60 -0.05 125.000 99.00 99.00
A 19.3 0.0032 138000 0 2 0
0.01 12.45 10.50 48.70 1.60 -0.04 111.300 120.20 120.20
A 19.43 0.0032 138000 0 2 0
0.04 39.00 84.86 144.67 1.60 -0.02 125.000 112.60 112.60
A 20.01 0.0032 138000 0 2 0
0.02 43.77 38.23 216.39 1.40 -0.04 109.500 99.00 99.00
A 19.44 0.0032 138000 0 2 0
6.56 536.20 274.89 0.00 32.20 -0.44 205.800 82.20 82.20
Z 15.94 19.3188 165000 3 2 0
12.61 1229.08 353.80 0.00 26.00 -0.37 188.600 89.60 89.60
Z 15.82 19.3188 165000 3 2 0
3.30 454.90 156.61 0.00 22.60 -0.32 169.200 84.80 84.80
Z 15.85 19.3188 165000 3 2 0
2.79 385.56 285.13 0.00 19.70 -0.25 164.300 88.40 88.40
Z 16.05 19.3188 165000 3 2 0
```

```
17-OJ-06
0 0 428
1 0 0 0 0 0
105
0 2 0
1 16.3
0
0
1
83 17 5 4.99
0.00 0
0.00 0
0.000 0
8
7
0.03 20.14 15.36 112.89 1.70 -0.02 170.500 129.40 129.40
A 19.38 0.0032 138000 0 2 0
0.02 14.59 31.54 125.78 1.40 -0.03 139.600 137.00 137.00
A 19.97 0.0032 138000 0 2 0
0.02 19.07 64.55 158.60 1.20 -0.02 171.800 105.20 105.20
A 20.33 0.0032 138000 0 2 0
0.01 16.57 36.30 49.36 1.00 -0.03 114.000 120.20 120.20
A 20.02 0.0032 138000 0 2 0
5.49 182.40 103.96 0.00 29.50 -0.38 231.000 126.40 126.40
Z 15.97 19.3188 165000 3 2 0
25.82 1056.82 404.10 0.00 26.90 -0.37 283.100 110.00 110.00
Z 15.87 19.3188 165000 3 2 0
11.72 1026.34 336.82 0.00 15.40 -0.22 206.700 117.00 117.00
Z 15.84 19.3188 165000 3 2 0
16.51 1146.64 380.60 0.00 8.60 -0.12 340.600 137.00 137.00
Z 15.85 19.3188 165000 3 2 0
```

```
17-OJ-07
1 1 901
1 25 20 350 1.6533e+06 6613
105
3 0.043 0.041
1 16.3
0
0
1
47 9 5 4.99
1.95 0.59
13.98 1.398
1.656 0.1656
0 38 0.16
0 98 0.03
0 21 0.01
0 41 0.02
0 21 0
1 15 0
1 92 0.08
1 33 0.08
1 128 0.08
0 48 0.09
0 41 0.09
0 130 0.03
0 15 0.02
1 58 0.02
1 82 0.05
1 59 0.02
0 22 0
1 188 0.01
2 254 0.06
1 247 0.02
14.18 0.0435
14.86 0.0435
14.6 0.0435
14.4 0.0435
14.82 0.0435
14.17 0.0435
14.84 0.0435
14.01 0.0435
14.74 0.0435
14.77 0.0435
14.9 0.0435
14.78 0.0435
15.37 0.0435
15.3 0.0435
15.21 0.0435
15.3 0.0435
16.25 0.0435
```

```
9.22 0.0435
10.58 0.0435
10.72 0.0435
12.81 0.0435
12.99 0.0435
13.81 0.0435
13.02 0.0435
13.76 0.0435
7
7
0.07 49.89 118.48 242.59 2.30 -0.03 98.500 121.60 121.60
A 20.07 0.0032 138000 0 2 0
0.02 24.51 27.32 34.46 1.30 -0.02 112.200 122.00 122.00
A 19.6 0.0032 138000 0 2 0
0.03 76.63 213.50 88.04 0.90 -0.01 85.200 108.20 108.20
A 20.22 0.0032 138000 0 2 0
8.71 892.92 167.08 0.00 18.20 -0.26 224.800 96.80 96.80
Z 15.76 19.3188 165000 3 2 0
9.06 883.27 676.18 0.00 17.20 -0.22 206.700 100.20 100.20
Z 16.07 19.3188 165000 3 2 0
3.98 368.50 162.32 0.00 10.80 -0.15 202.300 135.60 135.60
Z 15.9 19.3188 165000 3 2 0
1.46 388.42 112.06 0.00 8.80 -0.12 167.400 99.00 99.00
Z 15.82 19.3188 165000 3 2 0
```

```
17-OJ-08
0 0 1072
1 0 0 0 0 0
105
0 2 0
1 16.3
0
0
1
-47 -9 5 5
0.00 0
0.00 0
0.000 0
2
0
0.01 18.16 38.98 113.66 1.50 -0.03 79.100 95.80 95.80
A 19.98 0.0032 138000 0 2 0
0.01 41.08 82.19 114.01 1.10 -0.02 83.500 91.00 91.00
A 19.96 0.0032 138000 0 2 0
```

```
17-OJ-09
0 0 1892
1 0 0 0 0 0
105
0 2 0
1 16.3
0
0
1
36 2 5 4.99
0.00 0
0.00 0
0.000 0
7
7
0.02 35.32 66.96 124.32 1.60 -0.02 136.900 86.60 86.60
A 19.91 0.0032 138000 0 2 0
0.02 10.84 22.72 82.39 1.70 -0.03 151.900 115.80 115.80
A 19.96 0.0032 138000 0 2 0
0.02 26.98 58.53 65.10 1.40 -0.02 136.000 106.60 106.60
A 20.02 0.0032 138000 0 2 0
0.01 7.32 11.15 43.78 1.50 -0.03 158.600 123.20 123.20
A 19.74 0.0032 138000 0 2 0
16.48 2045.38 1252.12 0.00 26.70 -0.36 148.900 85.20 85.20
Z 15.99 19.3188 165000 3 2 0
7.30 339.10 154.02 0.00 27.50 -0.37 250.000 107.80 107.80
Z 15.91 19.3188 165000 3 2 0
12.27 1182.37 316.24 0.00 25.80 -0.37 173.600 94.60 94.60
Z 15.81 19.3188 165000 3 2 0
```

QTQt Data Files for Modeled Samples from the Sisar Canyon Transect
Vertical Sample Spacing Set by Present-Day Elevations

```
18-OSC-03
0 0 723
1 0 0 0 0 0
105
0 2 0
1 16.3
0
0
1
-41 -7 5 5
0.00 0
0.00 0
0.000 0
6
0
0.04 22.76 38.76 111.08 2.10 -0.03 176.700 118.80 118.80
A 19.83 6.0714e-5 122300 0 2 0
0.04 35.00 15.27 184.81 1.70 -0.03 182.900 116.60 116.60
A 19.18 6.0714e-5 122300 0 2 0
0.02 16.38 49.77 34.73 1.60 -0.02 146.200 105.20 105.20
A 20.28 6.0714e-5 122300 0 2 0
0.06 17.78 58.66 142.92 1.60 -0.02 211.600 146.20 146.20
A 20.31 6.0714e-5 122300 0 2 0
0.05 61.70 118.96 116.90 1.40 -0.02 164.300 97.20 97.20
A 19.94 6.0714e-5 122300 0 2 0
0.03 42.49 54.34 90.57 1.30 -0.02 170.500 104.60 104.60
A 19.67 6.0714e-5 122300 0 2 0
```

```
18-OSC-05
0 0 1085
1 0 0 0 0 0
105
0 2 0
1 16.3
0
0
1
-47 -9 5 5
0.00 0
0.00 0
0.000 0
6
0
0.01 6.27 21.40 265.84 2.60 -0.04 118.400 109.60 109.60
A 20.13 6.0714e-5 122300 0 2 0
0.10 92.87 78.82 274.00 2.30 -0.03 135.600 109.60 109.60
A 19.45 6.0714e-5 122300 0 2 0
0.02 11.66 45.62 411.69 2.00 -0.03 138.300 100.80 100.80
A 20.30 6.0714e-5 122300 0 2 0
0.01 3.75 15.29 213.07 2.10 -0.03 168.700 135.60 135.60
A 20.22 6.0714e-5 122300 0 2 0
0.01 11.90 35.38 148.85 1.80 -0.02 94.500 106.40 106.40
A 20.20 6.0714e-5 122300 0 2 0
0.03 59.31 91.70 62.40 1.60 -0.02 121.500 91.00 91.00
A 19.79 6.0714e-5 122300 0 2 0
```

```
18-OSC-07
0 0 1928
1 0 0 0 0 0
105
0 2 0
1 16.3
0
0
1
-41 -7 5 5
0.00 0
0.00 0
0.000 0
6
0
0.03 17.39 40.30 143.57 3.30 -0.04 136.900 104.60 104.60
A 20.03 6.0714e-5 122300 0 2 0
0.02 38.80 9.07 34.29 2.60 -0.04 112.200 88.00 88.00
A 19.09 6.0714e-5 122300 0 2 0
0.05 34.47 153.86 504.40 2.30 -0.03 112.700 100.80 100.80
A 20.53 6.0714e-5 122300 0 2 0
0.02 35.40 25.61 88.45 2.10 -0.03 112.600 83.60 83.60
A 19.38 6.0714e-5 122300 0 2 0
0.03 26.22 29.43 22.15 2.30 -0.03 117.500 115.20 115.20
A 19.60 6.0714e-5 122300 0 2 0
0.01 6.17 32.02 283.74 2.10 -0.04 108.700 105.20 105.20
A 20.51 6.0714e-5 122300 0 2 0
```

```
18-OSC-10
0 0 1606
1 0 0 0 0 0
105
0 2 0
1 16.3
0
0
1
-47 -9 5 5
0.00 0
0.00 0
0.000 0
3
0
0.02 29.60 28.56 159.55 2.60 -0.04 94.500 97.20 97.20
A 19.49 6.0714e-5 122300 0 2 0
0.06 100.68 130.76 729.99 2.40 -0.03 109.500 82.20 82.20
A 19.64 6.0714e-5 122300 0 2 0
0.02 22.37 11.30 70.36 2.50 -0.04 124.600 91.40 91.40
A 19.25 6.0714e-5 122300 0 2 0
```

QTQt Data File for Modeled Sample from the Santa Paula Canyon Transect

```
16SP-03
0 0 342
1 0 0 0 0 0
105
0 2 0
1 16.3
0
0
1
36 2 5 4.99
0.00 0
0.00 0
0.000 0
8
7
0.03 36.81 23.57 140.63 1.80 -0.03 155.000 91.40 91.40
A 19.32 6.0714e-5 122300 0 2 0
0.02 28.55 39.94 47.79 1.70 -0.05 126.300 106.40 106.40
A 19.72 6.0714e-5 122300 0 2 0
0.09 97.68 102.46 81.87 1.70 -0.02 144.900 109.20 109.20
A 19.57 6.0714e-5 122300 0 2 0
0.01 19.89 30.54 26.70 1.40 -0.08 108.200 106.80 106.80
A 19.79 6.0714e-5 122300 0 2 0
0.01 13.95 22.32 60.99 1.40 -0.08 108.200 112.20 112.20
A 19.79 6.0714e-5 122300 0 2 0
6.32 273.49 192.92 0.00 56.00 -0.69 144.000 100.20 100.20
Z 16.04 19.3188 165000 3 2 0
16.78 1213.37 298.82 0.00 37.60 -0.51 170.500 91.40 91.40
Z 15.80 19.3188 165000 3 2 0
3.51 393.86 148.65 0.00 32.90 -0.44 130.800 88.40 88.40
Z 15.87 19.3188 165000 3 2 0
```

QTQt Data Files for Modeled Samples from the Santa Paula Peak Transect
Vertical Sample Spacing Set by Present-Day Elevations

```
18-SPP-02
0 0 760
1 0 0 0 0 0
105
0 2 0
1 16.3
0
0
1
-41 -7 5 5
0.00 0
0.00 0
0.000 0
5
0
0.03 106.42 50.99 209.79 1.30 -0.02 89.700 85.20 85.20
A 19.24 6.0714e-5 122300 0 2 0
0.04 149.06 153.85 146.93 1.20 -0.01 95.900 85.20 85.20
A 19.56 6.0714e-5 122300 0 2 0
0.02 52.56 163.39 178.07 0.80 -0.01 98.900 86.60 86.60
A 20.29 6.0714e-5 122300 0 2 0
0.01 40.32 107.17 267.27 0.70 -0.02 112.600 82.20 82.20
A 20.15 6.0714e-5 122300 0 2 0
0.01 39.26 77.06 67.73 0.80 -0.01 100.700 89.60 89.60
A 19.95 6.0714e-5 122300 0 2 0
```

```
18-SPP-03
0 0 1512
1 0 0 0 0 0
105
0 2 0
1 16.3
0
0
1
-41 -7 5 5
0.00 0
0.00 0
0.000 0
6
0
0.02 19.62 31.52 126.79 2.60 -0.04 103.800 89.80 89.80
A 19.78 6.0714e-5 122300 0 2 0
0.08 106.59 176.55 189.00 2.30 -0.03 125.000 86.60 86.60
A 19.83 6.0714e-5 122300 0 2 0
0.04 34.53 38.52 58.31 2.10 -0.03 120.600 121.40 121.40
A 19.59 6.0714e-5 122300 0 2 0
0.02 34.30 21.21 36.18 2.00 -0.03 100.700 104.80 104.80
A 19.33 6.0714e-5 122300 0 2 0
0.04 45.66 67.39 71.35 1.70 -0.02 170.500 97.20 97.20
A 19.76 6.0714e-5 122300 0 2 0
0.01 22.38 48.10 91.63 1.30 -0.02 105.100 92.80 92.80
A 20.00 6.0714e-5 122300 0 2 0
```

```
18-SPP-06 Zr
0 0 936
1 0 0 0 0 0
105
0 2 0
1 16.3
0
0
1
41 7 5 5
0.00 0
0.00 0
0.000 0
4
3
26.31 981.71 145.98 0.00 46.40 -0.64 225.300 100.80 100.80
Z 15.74 19.3188 165000 3 2 0
37.43 686.95 449.12 0.00 48.90 -0.60 226.600 132.00 132.00
Z 16.01 19.3188 165000 3 2 0
35.09 896.67 310.66 0.00 43.00 -0.57 222.200 124.60 124.60
Z 15.85 19.3188 165000 3 2 0
6.43 604.69 99.60 0.00 21.00 -0.30 187.300 103.40 103.40
Z 15.75 19.3188 165000 3 2 0
```

QTQt Data Files for Modeled Samples from the Hopper Mountain Transect
Vertical Sample Spacing Set by Present-Day Elevations

```
16FM-01
0 0 264
1 0 0 0 0 0
105
0 2 0
1 16.3
0
0
1
-28.5 -5.5 5 5
0.00 0
0.00 0
0.000 0
5
0
0.04 76.48 9.73 259.93 1.60 -0.04 121.900 105.20 105.20
A 18.99 0.0032 138000 0 2 0
0.01 12.61 28.17 130.55 1.30 -0.03 146.200 101.60 101.60
A 19.98 0.0032 138000 0 2 0
0.02 26.92 29.28 221.49 1.30 -0.02 146.200 108.20 108.20
A 19.53 0.0032 138000 0 2 0
0.02 64.04 20.90 376.81 1.10 -0.02 86.600 99.00 99.00
A 19.10 0.0032 138000 0 2 0
0.03 72.16 159.81 98.02 1.00 -0.01 115.300 97.60 97.60
A 20.04 0.0032 138000 0 2 0
```

```
17-FC-01
0 0 353
1 0 0 0 0 0
105
0 2 0
1 16.3
0
0
1
-26.5 -1.5 5 5
0.00 0
0.00 0
0.000 0
4
0
0.01 16.99 37.58 301.89 1.60 -0.03 125.000 83.40 83.40
A 19.92 0.0032 138000 0 2 0
0.02 33.75 72.93 147.91 1.30 -0.02 127.700 86.60 86.60
A 20.00 0.0032 138000 0 2 0
0.01 30.97 64.63 350.25 1.00 -0.02 92.800 100.20 100.20
A 19.93 0.0032 138000 0 2 0
0.02 49.91 37.72 53.45 0.90 -0.01 169.200 89.60 89.60
A 19.41 0.0032 138000 0 2 0
```

```
17-FC-02
0 0 756
1 0 0 0 0 0
105
0 2 0
1 16.3
0
0
1
-28.5 -5.5 5 5
0.00 0
0.00 0
0.000 0
4
0
0.02 30.41 33.97 400.55 2.00 -0.03 126.300 89.60 89.60
A 19.50 0.0032 138000 0 2 0
0.04 32.72 175.58 335.11 1.60 -0.02 121.900 95.80 95.80
A 20.71 0.0032 138000 0 2 0
0.02 15.99 45.59 102.06 1.10 -0.02 162.500 131.20 131.20
A 20.20 0.0032 138000 0 2 0
0.01 17.48 114.22 172.18 0.90 -0.02 121.500 83.60 83.60
A 20.88 0.0032 138000 0 2 0
```

```
17-FC-03
0 0 671
1 0 0 0 0 0
105
0 2 0
1 16.3
0
0
1
-19.5 -3.5 5 5
0.00 0
0.00 0
0.000 0
4
0
0.01 12.48 23.99 99.48 1.50 -0.02 153.700 99.40 99.40
A 19.89 0.0032 138000 0 2 0
0.02 23.53 78.74 142.33 1.30 -0.02 163.000 95.40 95.40
A 20.34 0.0032 138000 0 2 0
0.01 27.43 42.15 198.49 1.20 -0.02 129.400 91.40 91.40
A 19.74 0.0032 138000 0 2 0
0.01 23.25 107.66 198.81 1.10 -0.02 97.200 85.20 85.20
A 20.60 0.0032 138000 0 2 0
```

```
17-FC-04
0 0 552
1 0 0 0 0 0
105
0 2 0
1 16.3
0
0
1
-19.5 -3.5 5 5
0.00 0
0.00 0
0.000 0
3
0
0.02 11.22 62.28 151.48 1.70 -0.02 123.300 122.00 122.00
A 20.73 0.0032 138000 0 2 0
0.01 9.81 14.65 80.03 1.40 -0.02 159.900 120.60 120.60
A 19.72 0.0032 138000 0 2 0
0.02 23.74 55.29 68.93 1.10 -0.01 142.700 124.60 124.60
A 20.07 0.0032 138000 0 2 0
```

```
18-FC-01
0 0 1263
1 0 0 0 0 0
105
0 2 0
1 16.3
0
0
1
-10.6 -5.3 5 5
0.00 0
0.00 0
0.000 0
5
0
0.03 23.12 58.42 24.97 3.10 -0.03 115.300 97.20 97.20
A 20.14 0.0032 138000 0 2 0
0.02 25.11 11.90 360.41 2.80 -0.04 115.300 97.20 97.20
A 19.12 0.0032 138000 0 2 0
0.02 17.50 12.90 247.81 2.40 -0.04 133.800 97.20 97.20
A 19.29 0.0032 138000 0 2 0
0.01 5.06 16.09 60.87 2.30 -0.03 110.000 127.60 127.60
A 20.26 0.0032 138000 0 2 0
0.03 29.64 80.96 110.04 2.10 -0.03 145.800 94.60 94.60
A 20.19 0.0032 138000 0 2 0
```

```
18-FC-02
0 0 1142
1 0 0 0 0 0
105
0 2 0
1 16.3
0
0
1
-10.6 -5.3 5 5
0.00 0
0.00 0
0.000 0
4
0
0.01 13.25 53.94 162.13 1.60 -0.02 91.400 100.80 100.80
A 20.47 0.0032 138000 0 2 0
0.01 19.02 34.87 49.45 1.50 -0.03 106.500 92.40 92.40
A 19.90 0.0032 138000 0 2 0
0.02 16.88 138.40 51.03 1.60 -0.02 118.800 100.20 100.20
A 21.09 0.0032 138000 0 2 0
0.02 29.15 86.21 87.35 1.00 -0.01 204.100 89.60 89.60
A 20.26 0.0032 138000 0 2 0
```

QTQt Data Files for Modeled Samples from the Santa Rosa Island Transect
Vertical Sample Spacing Set by Stratigraphic Separation

```
18-SRI-05
0 0 874
1 0 0 0 0 0
105
0 2 0
1 16.3
0
0
1
-19.5 -3.5 5 5
0.00 0
0.00 0
0.000 0
4
0
0.15 41.67 131.12 109.01 6.90 -0.07 137.400 92.40 92.40
A 20.31 6.0714e-5 122300 0 2 0
0.05 22.68 20.01 24.40 6.50 -0.10 95.900 108.20 108.20
A 19.48 6.0714e-5 122300 0 2 0
0.04 35.27 30.64 178.41 4.90 -0.07 106.900 79.20 79.20
A 19.44 6.0714e-5 122300 0 2 0
0.02 18.06 27.17 15.26 3.80 -0.27 95.000 85.20 85.20
A 19.78 6.0714e-5 122300 0 2 0
```

```
18-SRI-06
0 0 283
1 0 0 0 0 0
105
0 2 0
1 16.3
0
0
1
-43 -5 5 5
0.00 0
0.00 0
0.000 0
6
0
0.04 14.08 25.21 33.09 5.10 -0.07 149.300 103.80 103.80
A 19.88 6.0714e-5 122300 0 2 0
0.07 27.37 53.18 47.96 4.80 -0.06 166.100 94.00 94.00
A 19.94 6.0714e-5 122300 0 2 0
0.02 9.76 23.05 65.08 4.80 -0.07 125.900 95.80 95.80
A 20.05 6.0714e-5 122300 0 2 0
0.06 20.13 62.32 168.70 4.70 -0.09 165.600 89.60 89.60
A 20.26 6.0714e-5 122300 0 2 0
0.05 14.04 24.41 34.79 5.10 -0.06 112.600 132.00 132.00
A 19.86 6.0714e-5 122300 0 2 0
0.06 15.60 26.91 39.99 4.90 -0.06 175.800 109.60 109.60
A 19.85 6.0714e-5 122300 0 2 0
```

```
18-SRI-07
0 0 397
1 0 0 0 0 0
105
0 2 0
1 16.3
0
0
1
-25.5 -2.5 5 5
0.00 0
0.00 0
0.000 0
5
0
0.05 13.58 24.34 42.26 6.70 -0.08 196.100 86.60 86.60
A 19.88 6.0714e-5 122300 0 2 0
0.16 115.83 11.25 150.70 5.80 -0.09 118.800 88.40 88.40
A 18.99 6.0714e-5 122300 0 2 0
0.04 9.51 17.23 24.52 6.10 -0.08 128.100 114.00 114.00
A 19.89 6.0714e-5 122300 0 2 0
0.10 29.60 76.42 94.11 5.30 -0.06 159.400 97.60 97.60
A 20.15 6.0714e-5 122300 0 2 0
0.03 13.12 34.91 225.53 4.50 -0.08 129.000 89.80 89.80
A 20.08 6.0714e-5 122300 0 2 0
```

```
18-SRI-10
0 0 647
1 0 0 0 0 0
105
0 2 0
1 16.3
0
0
1
-25.5 -5.5 5 5
0.00 0
0.00 0
0.000 0
6
0
0.05 15.93 27.46 267.23 7.00 -0.08 120.100 99.00 99.00
A 19.75 6.0714e-5 122300 0 2 0
0.05 16.34 29.35 42.63 6.20 -0.08 178.000 89.60 89.60
A 19.88 6.0714e-5 122300 0 2 0
0.07 59.64 40.39 230.15 5.40 -0.07 103.400 83.40 83.40
A 19.34 6.0714e-5 122300 0 2 0
0.10 53.83 78.68 134.73 5.60 -0.07 102.000 97.60 97.60
A 19.75 6.0714e-5 122300 0 2 0
0.06 26.80 8.02 245.57 5.60 -0.08 118.400 109.60 109.60
A 19.06 6.0714e-5 122300 0 2 0
0.02 16.03 14.15 203.41 4.20 -0.06 101.600 86.60 86.60
A 19.38 6.0714e-5 122300 0 2 0
```

QTQt Data Files for Modeled Samples from the Hollywood Transect
Vertical Sample Spacing Set by Stratigraphic Separation

```
16NC-01
0 0 1
1 0 0 0 0 0
105
0 2 0
1 16.3
0
0
1
-105 -3.2 530 40
0.00 0
0.00 0
0.000 0
7
7
0.12 133.52 89.15 116.07 2.30 -0.03 192.200 85.20 85.20
A 19.36 0.0032 138000 0 2 0
0.07 80.33 94.92 162.32 2.30 -0.03 100.300 107.80 107.80
A 19.62 0.0032 138000 0 2 0
0.09 119.92 105.40 138.52 2.10 -0.03 160.300 88.40 88.40
A 19.48 0.0032 138000 0 2 0
8.46 659.39 159.13 0.00 19.70 -0.26 251.300 100.20 100.20
Z 15.79 19.3188 165000 3 2 0
5.79 674.18 183.49 0.00 17.30 -0.23 216.100 94.00 94.00
Z 15.81 19.3188 165000 3 2 0
7.59 500.68 137.76 0.00 17.40 -0.23 280.400 109.60 109.60
Z 15.81 19.3188 165000 3 2 0
8.93 1300.15 240.20 0.00 13.80 -0.19 214.700 95.40 95.40
Z 15.76 19.3188 165000 3 2 0
```

```
17-HW-01
0 0 1755
1 0 0 0 0 0
105
0 2 0
1 16.3
0
0
1
-13.8 -2.2 5 4.99
0.00 0
0.00 0
0.000 0
4
0
0.03 9.59 8.78 279.87 6.60 -0.09 153.700 103.40 103.40
A 19.26 0.0032 138000 0 2 0
0.06 27.51 47.89 115.97 5.70 -0.07 172.300 82.20 82.20
A 19.85 0.0032 138000 0 2 0
0.08 37.91 48.06 112.78 5.20 -0.06 167.000 86.60 86.60
A 19.66 0.0032 138000 0 2 0
0.02 14.80 19.19 366.38 3.70 -0.05 112.600 100.20 100.20
A 19.49 0.0032 138000 0 2 0
```

```
17-HW-02
0 0 1980
1 0 0 0 0 0
105
0 2 0
1 16.3
0
0
1
-13.8 -2.2 5 4.99
0.00 0
0.00 0
0.000 0
2
0
0.10 29.94 21.95 226.65 6.80 -0.09 138.200 109.60 109.60
A 19.34 0.0032 138000 0 2 0
0.05 14.88 43.41 170.51 6.40 -0.08 129.000 101.60 101.60
A 20.19 0.0032 138000 0 2 0
```

```
17-HW-03
0 0 855
1 0 0 0 0 0
105
0 2 0
1 16.3
0
0
1
-105 -3.2 530 40
0.00 0
0.00 0
0.000 0
4
0
0.05 40.98 25.91 125.97 3.80 -0.08 167.400 84.80 84.80
A 19.32 0.0032 138000 0 2 0
0.08 53.17 26.35 149.47 3.60 -0.05 150.600 99.00 99.00
A 19.24 0.0032 138000 0 2 0
0.08 35.83 18.80 108.92 3.50 -0.05 173.600 111.40 111.40
A 19.26 0.0032 138000 0 2 0
0.04 37.90 17.81 103.34 3.10 -0.04 171.800 87.00 87.00
A 19.23 0.0032 138000 0 2 0
```

```
17-HW-04
0 0 1020
1 0 0 0 0 0
105
0 2 0
1 16.3
0
0
1
-83 -17 5 4.99
0.00 0
0.00 0
0.000 0
4
0
0.16 53.67 28.89 203.17 5.97 -0.08 138.700 114.00 114.00
A 19.26 0.0032 138000 0 2 0
0.20 61.53 52.98 170.19 4.40 -0.05 170.500 121.40 121.40
A 19.45 0.0032 138000 0 2 0
0.02 7.12 16.63 129.22 7.99 -0.10 133.900 83.40 83.40
A 19.45 0.0032 138000 0 2 0
0.0672 20.45 26.25 157.86 7.68 -0.09 121.5 103.4 103.4
A 19.45 0.0032 138000 0 2 0
```

```
17-HW-06
0 0 2476
1 0 0 0 0 0
105
0 2 0
1 16.3
0
0
1
-13.8 -2.2 5 4.99
0.00 0
0.00 0
0.000 0
4
0
0.07 22.11 14.36 362.87 9.70 -0.13 161.200 82.20 82.20
A 19.22 0.0032 138000 0 2 0
0.07 25.43 51.44 233.87 5.90 -0.07 146.200 89.60 89.60
A 19.92 0.0032 138000 0 2 0
0.06 18.84 14.62 288.13 5.70 -0.07 151.900 114.00 114.00
A 19.30 0.0032 138000 0 2 0
0.02 7.28 24.95 124.41 4.90 -0.06 112.200 109.60 109.60
A 20.29 0.0032 138000 0 2 0
```